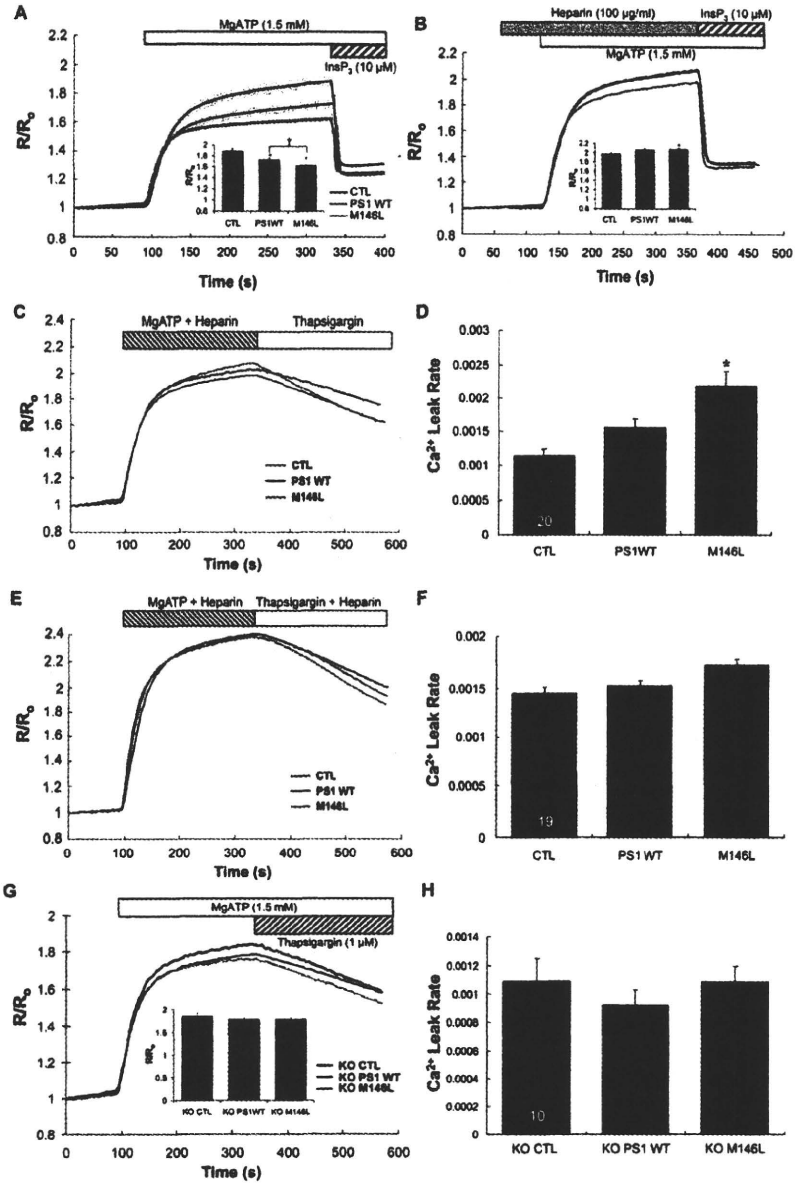

Figure 6. The Amount of Ca^{2+} in the ER Store Is Not Increased by PS1-M146L Expression, Due to FAD Mutant PS1- and $InsP_3R$-Dependent Enhanced Ca^{2+} Leak Permeability of the ER Membrane

(A) ER $[Ca^{2+}]$ expressed as Mag-Fura-2 ratio normalized to ratio at t = 0 before and then during filling upon addition of MgATP (1.5 mM) and subsequent emptying by addition of $InsP_3$ (10 μM) in control (blue) and PS1-WT (red) and PS1-M146L (green) stable DT40 cells. Insert: Steady-state ER $[Ca^{2+}]$ in presence of MgATP. Asterisks: $p < 0.01$ compared with control cells. Cross: $p < 0.01$ compared with PS1-WT.

(B) Similar experiment with ER Ca^{2+} loading performed in presence of heparin (100 μg/ml). Asterisk: $p < 0.01$ and < 0.05 compared with control and PS1-WT cells, respectively.

(C) ER $[Ca^{2+}]$ during filling upon addition of MgATP (1.5 mM) in presence of heparin (100 μg/ml) and then after removal of MgATP and addition of thapsigargin (1 μM), in control (blue), and PS1-WT (red) and PS1-M146L (green) stable DT40 cells.

(D) Summary of ER Ca^{2+} leak rate, calculated as initial rate of decline of the Mag-Fura-2 ratio. Asterisk: enhanced leak observed in M146L-expressing cells compared with control and PS1-WT ($p < 0.01$).

(E) Similar experiments as in (D), except that heparin (100 μg/ml) was present during measurements of the Ca^{2+} leak rate.

(F) Summary of ER Ca^{2+} leak rate in presence of heparin.

(G) Similar experiment as in (D) performed in cells lacking $InsP_3R$ expression (KO). Insert: steady-state ER $[Ca^{2+}]$ after MgATP-induced loading.

(H) Summary of ER Ca^{2+} leak rate in PS1 expressing $InsP_3R$ KO cells.

Bars indicate standard error of the mean.

suggest that mutant PS1-M146L diminishes the size of the ER Ca^{2+} store by a mechanism that involves its enhancement of $InsP_3R$ channel activity, a process that disrupts the normal Ca^{2+} pump/leak balance in favor of enhanced leak mediated by $InsP_3$-dependent $InsP_3R$-mediated Ca^{2+} permeability. We conclude, therefore, that the observed altered $InsP_3R$ single-channel activity most likely accounts for the altered $[Ca^{2+}]_i$ signals observed.

FAD Mutant PS1 Enhances $InsP_3R$-Mediated ER Ca^{2+} Permeability in Brain Neurons

Whereas FAD mutant PS associated exaggerated Ca^{2+} signaling has been observed in many cell types, AD pathophysiology is manifested primarily in brain neurons. To determine if FAD PS1 expression was associated with altered $InsP_3R$-mediated Ca^{2+} release in brain neurons, cortical neurons were isolated from E15–E16 mouse brains, and the Ca^{2+} permeability properties of the ER membranes were measured as above (Figure 7A). The steady-state level of Ca^{2+} accumulated in the ER lumen was not different between control cells and neurons expressing either WT or M146L-PS1 (Figure 7B). The Ca^{2+} leak permeability measured upon addition of thapsigargin was somewhat higher in PS1-M146L expressing neurons than in those expressing PS1-WT ($p < 0.05$), although it was not different compared with control cells (Figure 7C). In a separate set of experiments (Figure 7D), 33 nM $InsP_3$ failed to elicit Ca^{2+} release in control or PS1-WT cells, whereas it simulated Ca^{2+} release from the ER of PS1-M146L cells (Figure 7E), with an initial rate that was comparable to that achieved by addition of saturating (10 μM) $InsP_3$ to the control cells (Figure 7F). Thus, as in the non-neuronal cells examined, FAD mutant PS1 specifically sensitizes $InsP_3R$-mediated Ca^{2+} release in brain cortical neurons.

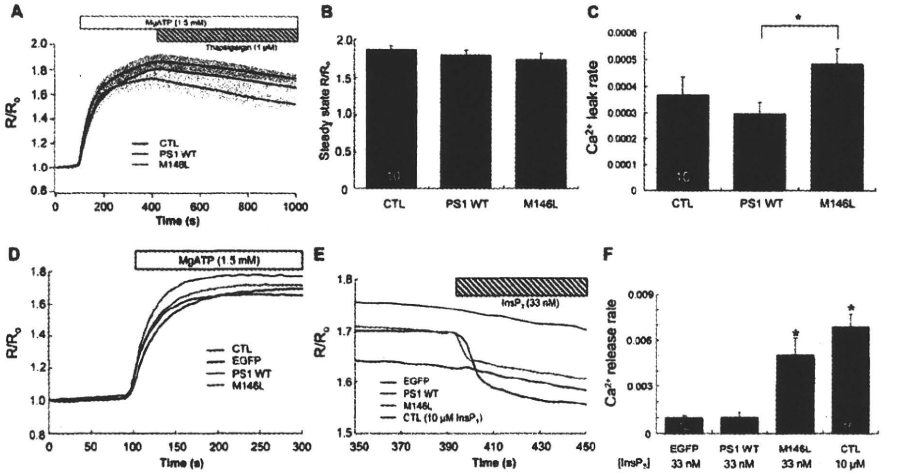

Figure 7. FAD Mutant PS1 Enhances $InsP_3R$-Mediated ER Ca^{2+} Permeability in Brain Neurons

(A) ER $[Ca^{2+}]$, expressed as Mag-Fura-2 ratio normalized to ratio at t = 0, before and then during filling upon addition of MgATP (1.5 mM), and subsequent exposure to 1 μM thapsigargin in control (blue) and PS1-WT (red)- and PS1-M146L (green)-transfected mouse cortical neurons.

(B) Summary of steady-state ER $[Ca^{2+}]$ following MgATP-induced loading in (A).

(C) Summary of Ca^{2+} leak rate measured in presence of thapsigargin in (A). Asterisk: p = 0.01.

(D) ER $[Ca^{2+}]$ during filling upon addition of MgATP (1.5 mM) in control (black) and EGFP (blue)-, PS1-WT (red)-, and PS1-M146L (green)-transfected mouse cortical neurons.

(E) Response of ER $[Ca^{2+}]$ to 33 nM $InsP_3$ in cells from (D) and in control cells in response to 10 μM $InsP_3$ (black trace).

(F) Summary of initial Ca^{2+} release rate, expressed as Mag-Fura-2 ratio, from (E).

Asterisks: p < 0.01 compared with control and PS1-WT. Bars indicate standard error of the mean.

Functional Consequences of $InsP_3R$-PS1 Interaction—APP Processing

Identification of a molecular mechanism that links FAD mutant PS to altered $[Ca^{2+}]_i$ signaling provides an opportunity for insights into relationships between pathological features of AD and altered $[Ca^{2+}]_i$ signaling. PS1 is the core subunit of the γ-secretase that enzymatically cleaves APP into amyloid peptides, including $A\beta_{40}$ and $A\beta_{42}$ (Edbauer et al., 2003). FAD PS mutations alter secretase function by either modifying its sequence specificity or absolute activity, such that the relative proportion or amount of $A\beta_{42}$ produced is increased (Citron et al., 1997; Scheuner et al., 1996). To determine the relevance of the functional interaction of PS1 and $InsP_3R$ for APP processing, we engineered DT40 cells to stably express APP harboring Swedish mutations (APP_{SWE}) that enhance production of Aβ species (Scheuner et al., 1996), together with either PS1-WT or PS1-M146L (Figure 8A). PS1-M146L specifically enhanced $A\beta_{40}$ and $A\beta_{42}$ by ~2- and ~3-fold, respectively, compared with control cells. This result is consistent with observations in other cell types (Citron et al., 1997), validating again the use of this model system. Of note, the $A\beta_{42}/A\beta_{40}$ ratio was enhanced in the FAD mutant PS1-expressing cells (Figure 8), as observed in AD patients. To determine the role of the $InsP_3R$ in PS1-dependent APP processing, APP and PS1-expxressing cells were generated in the $InsP_3R$-KO background, and APP processing was similarly evaluated. Remarkably, the mutant PS1 enhancement of Aβ secretion observed in the $InsP_3R$-expressing cells was abolished. Furthermore, the absolute levels of Aβ peptides detected were strongly reduced in all control and PS1-expressing $InsP_3R$-KO lines (Figure 8B). These results indicate that altered APP processing by mutant PS1-M146L PS1 has a strong dependence on the $InsP_3R$.

DISCUSSION

The underlying pathogenic mechanisms of Alzheimer's disease remain obscure. In this study, we considered that dysregulated $[Ca^{2+}]_i$ signaling is a proximal mechanism in AD. We used non-neuronal model cell systems because they provided unique advantages for deciphering the molecular mechanisms involved and confirmed the major results in primary brain neurons. Both the $InsP_3R$ (Foskett et al., 2007) as well as presenilins (Hebert et al., 2004) are widely distributed throughout all tissues investigated, with the highest levels of PS expression outside the brain (Hebert et al., 2004), and similar Ca^{2+} signaling abnormalities have been observed in several peripheral and neuronal cell types that express mutant PS (LaFerla, 2002; Smith et al., 2005a; Stutzmann, 2005). We have demonstrated that FAD mutant presenilins interact biochemically and functionally with the $InsP_3R$ Ca^{2+} release channel and exert profound stimulatory effects on its gating activity that result in exaggerated Ca^{2+} signaling in intact cells, including brain neurons. Our results indicate that this functional interaction has physiological implications that may be relevant in AD, including APP processing.

Presenilins Regulate $InsP_3R$ Ca^{2+} Release Channel Gating

We observed that expression of two FAD mutant PS (PS1-M146L and PS2-N141I) each had strong and similar effects on

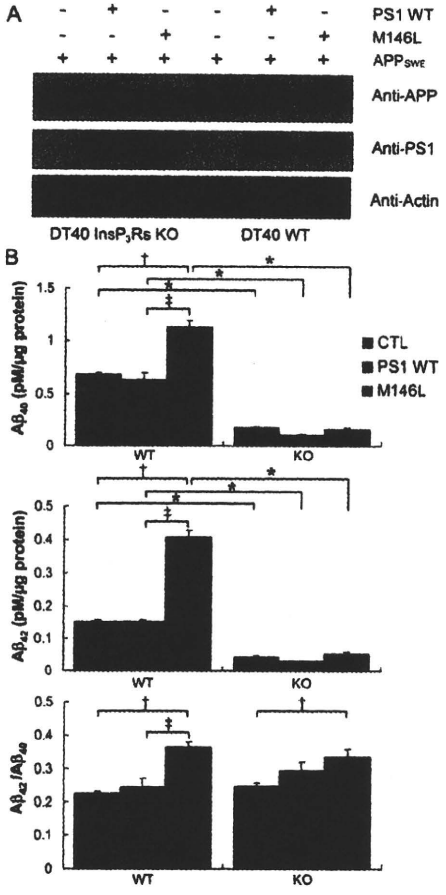

Figure 8. APP Processing Is Dependent on $InsP_3R$

(A) Stable expression of PS1-WT and PS1-M146L proteins in wild-type (WT) and $InsP_3R$-deficient (KO) DT40 cell lines that stably expressed APP_{SWE}. Actin probed as loading control.

(B) ELISA measurements of $A\beta_{40}$ (top), $A\beta_{42}$ (middle), and $A\beta_{42}/A\beta_{40}$ ratio (bottom) secreted over 48 hr by $InsP_3R$-expressing wild-type (WT; left) or $InsP_3R$-deficient (KO DT40 cells; right) DT40 cells stably expressing APP_{SWE} alone (blue) or APP_{SWE} with PS1-WT (red) or PS1-M146L (green).

Bars indicate standard error of the mean. Asterisks: $p < 0.01$ compared with control WT cells. Cross: $p < 0.01$ compared with control WT cells; double cross: $p < 0.01$ compared with PS1-WT cells.

the gating of single $InsP_3R$ Ca^{2+} release channels. We attempted to ensure equal levels of expression of $InsP_3R$ and the different PS proteins among the different groups of cells, but this could not be achieved perfectly. Nevertheless, because very similar results were obtained in two very distinct cell systems, Sf9 and DT40 cells, this was likely not a significant confounding variable. In both systems, mutant PS expression caused the $InsP_3R$ channel to gate as actively in low submaximal [$InsP_3$] as it normally does in saturating [$InsP_3$]. Elevated P_o in low [$InsP_3$] by FAD mutant PS was caused primarily by a substantial increase of channel opening rate, the major mechanism whereby $InsP_3$ activates the channel (Foskett et al., 2007), indicating that mutant PS enhances $InsP_3R$ gating by sensitizing it to low [$InsP_3$]. This mechanism is likely an allosteric one mediated by interaction of PS with the $InsP_3R$ that is preserved in isolated nuclei. Both membrane proteins localized to the nuclear envelope and mutant- as well as WT-PS coimmunoprecipitated to the same extent with mammalian $InsP_3R$, suggesting that PS mutations do not strongly affect the biochemical interaction. Although WT PS1 or PS2 did not affect channel P_o, small effects on $InsP_3R$ channel gating were nevertheless observed. It has been debated whether FAD PS mutations are gain or loss of function (Shen and Kelleher, 2007). Here, we show an apparent gain in $InsP_3R$ function by FAD mutant PS expression. However, channel dwell time analyses suggest that WT PS1 and PS2 also influence $InsP_3R$ channel gating. It is possible therefore that the gain-of-function phenotype we observe is due to disruption by mutant PS of normal PS-WT regulation of $InsP_3R$ channel activity. Future studies of the $InsP_3R$ gating behaviors in PS-deficient cells will be informative in this regard.

FAD Mutant PS1-Mediated Enhanced $InsP_3R$ Gating Causes Exaggerated $[Ca^{2+}]_i$ Signaling

Analysis of our single-channel data suggests that mutant PS1 and PS2 stimulate $InsP_3R$ gating by sensitizing the channel to $InsP_3$. One of the most consistent observations of the effects of FAD PS on Ca^{2+} signaling is potentiation of $InsP_3$-mediated Ca^{2+} release (Smith et al., 2005a; Yoo et al., 2000). Nevertheless, the molecular mechanisms have remained obscure. $InsP_3$-mediated $[Ca^{2+}]_i$ signals in FAD patient fibroblasts were exaggerated in response to low agonist concentrations (Ito et al., 1994), consistent with an enhanced sensitivity to $InsP_3$ in AD. The magnitude and rate of $[Ca^{2+}]_i$ rise in response to photo-release of $InsP_3$ were enhanced by FAD mutant PS in *Xenopus* oocytes (Leissring et al., 1999a, 1999b). Furthermore, Ca^{2+} puffs, low-level Ca^{2+} release events mediated by clusters of $InsP_3R$ in response to submaximal [$InsP_3$], were both more frequent and likely to generate $[Ca^{2+}]_i$ waves in the FAD mutant PS-expressing cells (Leissring et al., 2001). In brain slices from PS1-M146V knockin mice, photo-release of $InsP_3$ caused 3-fold greater Ca^{2+} release than in nontransgenic neurons and enhanced the number of neurons responding and those exhibiting strong responses (Stutzmann et al., 2004). By demonstrating that mutant PS sensitizes the $InsP_3R$ to $InsP_3$, our new results provide a molecular mechanism that is consistent with these previous observations and can therefore possibly account for them. To test this idea, the relevance of the observed effects of FAD PS1 expression on $InsP_3R$ single-channel gating was determined by measuring $[Ca^{2+}]_i$ responses in PS-expressing DT40 cells, the same cells used for the single-channel studies, that had comparable levels of $InsP_3R$ expression. Exaggerated Ca^{2+} release responses to both high- as well as low-threshold concentrations of agonist were observed in the cells that expressed the PS1-M146L protein. In a significant proportion of the FAD mutant PS-expressing cells, the $[Ca^{2+}]_i$ responses to low agonist concentrations mimicked the responses of normal cells to a saturating agonist concentration. Furthermore, a high percentage of PS1-M146L-expressing unstimulated cells displayed spontaneous low-level $[Ca^{2+}]_i$ signals in the absence of agonist stimulation. Most importantly, the exaggerated Ca^{2+} responses were mediated specifically by the $InsP_3R$, since they were absent in

$InsP_3R$ knockout cells. All these features are consistent with an enhanced $InsP_3$ sensitivity of the $InsP_3R$ in intact cells expressing FAD mutant PS, even to [$InsP_3$] that may exist in resting, unstimulated cells. The conclusions based on the effects of PS1-M146L expression on $[Ca^{2+}]_i$ signals are therefore in strong agreement with those reached from the single-channel studies. Thus, these results suggest that exaggerated $[Ca^{2+}]_i$ signals in cells can be accounted for by exaggerated $InsP_3R$ gating as a result of its interaction with FAD mutant PS. Importantly, these insights appear to be relevant for brain neurons, since $InsP_3R$-mediated ER Ca^{2+} permeability was enhanced by FAD mutant PS1 expression in mouse brain cortical neurons, enabling Ca^{2+} release to be triggered by low [$InsP_3$] that were without effect in either control cells or cells expressing WT PS1.

It has been suggested that exaggerated Ca^{2+} release in AD cells is due to increased filling of ER Ca^{2+} stores (discussed in LaFerla, 2002; Mattson and Chan, 2003; Stutzmann, 2005). Although this "Ca^{2+} overload" hypothesis has been widely invoked, many studies, including ours here, have observed either no alteration or reduced ER Ca^{2+} stores in FAD PS-expressing cells (Giacomello et al., 2005; Lessard et al., 2005; Zatti et al., 2004, 2006). The absence of elevated ER [Ca^{2+}] suggests that the effects of FAD PS on $InsP_3R$ gating observed here cannot be accounted for by possible effects of elevated luminal [Ca^{2+}] on channel function. Furthermore, we have observed in excised luminal side-out nuclear patches that $InsP_3R$ channel gating is insensitive to bath (luminal) [Ca^{2+}] between 100 nM and 500 μM (data not shown). Ca^{2+} release is affected by many variables, including activities and expression of release channels, amount of ER Ca^{2+}, Ca^{2+} buffering, and more. Enhanced spontaneous Ca^{2+} release activity observed in our PS1-M146L-expressing DT40 cells reduced ER Ca^{2+}, but $[Ca^{2+}]_i$ responses to agonists were nevertheless enhanced because of the strong effect of mutant PS on $InsP_3R$ gating. Thus, exaggerated Ca^{2+} release responses cannot provide unambiguous measurements of the amount of Ca^{2+} in stores. Our results demonstrate that effects of FAD mutant PS1 on both $[Ca^{2+}]_i$ signaling and ER Ca^{2+} content are $InsP_3R$ dependent, with mutant PS1- and PS2-stimulated $InsP_3R$ channels remaining regulated by $InsP_3$. Thus, cell type-specific differences in concentrations of $InsP_3R$ ligands and expression levels can contribute to the magnitude of the effect of mutant PS1 expression on ER Ca^{2+}, which might reconcile discrepant published observations. The enhanced Ca^{2+} release responses observed in PS1-M146L-expressing DT40 cells are highly reminiscent of those in peripheral and neuronal mutant PS-expressing cells in many previous studies. The absence of these responses in $InsP_3R$-knockout cells, together with the identification of a molecular mechanism observed at the single channel level, strongly suggest that mutant PS-mediated enhancement of $InsP_3$ sensitivity of the $InsP_3R$ is a fundamental underlying mechanism that accounts for many observations of dysregulated Ca^{2+} signaling in AD cells and model cell systems.

It has been reported that exaggerated Ca^{2+} responses in cells expressing FAD mutant PS are associated with enhanced expression or activities of ryanodine receptor (RyR) Ca^{2+} release channels (Chan et al., 2000; Smith et al., 2005b; Stutzmann et al., 2006). In AD-transgenic mouse cortical neurons, exaggerated responses to $InsP_3$ were mediated in part by RyR activated by Ca^{2+} released through $InsP_3R$ (Stutzmann et al., 2006), suggesting that exaggerated RyR responses could be a secondary effect. Because Ca^{2+} signaling can influence $InsP_3R$ (Cai et al., 2004; Genazzani et al., 1999) and RyR (P. Nicotera, personal communication) expression, it is possible that mutant PS-mediated enhanced $InsP_3R$ Ca^{2+} signaling drives transcriptional programs, with RyR expression upregulated as a result. Conversely, Aβ exposure increased RyR expression in mouse cortical neurons (Supnet et al., 2006), suggesting that changes in RyR expression may be more downstream compared with a more proximal $InsP_3R$-mediated process described here. Alternately, PS and RyR may functionally interact similar to the PS-$InsP_3R$ interaction. PS2 has been reported to interact with RyR2, the cardiac isoform, and PS2 knockout results in cardiac Ca^{2+} signaling abnormalities (Takeda et al., 2005). In addition, WT and mutant PS1 have been reported to interact with RyR3 (Chan et al., 2000).

It was proposed that reconstituted PS proteins form divalent cation-permeable ion channels in bilayer membranes and that loss of this function in FAD PS enhanced ER Ca^{2+}, resulting in exaggerated Ca^{2+} release responses (Nelson et al., 2007; Tu et al., 2006). In contrast, we did not detect in native ER membranes a cation permeability associated with either WT or FAD mutant PS expression. Furthermore, we found that FAD mutant PS expression either reduced (DT40 cells) or had no effect (cortical neurons) on the amount of Ca^{2+} in the ER. Thus, our experiments failed to discover evidence in support of the hypothesis that PS form ion channels.

Finally, it should be emphasized that the Ca^{2+} signaling abnormalities we observed represent proximal mechanisms distinct from effects of Aβ on Ca^{2+} signaling (Mattson and Guo, 1997). Our studies indicate the presence of a complex involving PS and $InsP_3R$ that results in hyperactivation of the Ca^{2+} release channel in a process that is independent of Aβ.

Enhanced PS-Dependent $InsP_3R$-Mediated Ca^{2+} Signaling Enhances Aβ Processing

Disrupted Ca^{2+} signaling in AD cells has been well documented, but its physiological implications and the roles that these changes play in AD pathogenesis have not been well studied. Altered Ca^{2+} signaling could impinge on synaptic plasticity, membrane excitability, oxidative stress, and APP processing. Identification of the $InsP_3R$ as a molecular mechanism of Ca^{2+} disruption associated with FAD PS now suggests specific hypotheses that can be tested to evaluate the relevance of altered Ca^{2+} signaling through this pathway on disease-associated processes.

Our data suggest that one function of PS proteins may be to regulate the activity of the $InsP_3R$. Is there a relationship between this activity and the activity of PS as secretases? APP processing can be enhanced by elevations of $[Ca^{2+}]_i$ (Buxbaum et al., 1994; Jolly-Tornetta et al., 1998; Querfurth and Selkoe, 1994) and diminished by inhibition of ER Ca^{2+} release (Buxbaum et al., 1994). APP processing was examined in DT40 cells lines engineered to stably express PS1 and APP_{SWE}, exploiting DT40 KO cells as the only cell type available that completely lacks $InsP_3R$ expression. Expression of PS1-M146L caused a nearly 3-fold increase in $A\beta_{42}$ compared with control and

PS1-WT-expressing cells. Consequently, $A\beta_{42}/A\beta_{40}$ increased ~2-fold, recapitulating an important feature of AD (Haass and Selkoe, 2007). Importantly, APP processing appeared to be strongly dependent on the $InsP_3R$, since production of $A\beta_{40}$ and $A\beta_{42}$ were substantially lower in $InsP_3R$-deficient lines. Furthermore, the PS1-M146L enhancement of $A\beta_{42}$ and $A\beta_{42}/A\beta_{40}$ were eliminated in the $InsP_3R$-KO cells. These results suggest that the γ-secretase activity of WT and FAD mutant PS may be regulated by either Ca^{2+} released through the $InsP_3R$, or their biochemical interaction with the channel. Our studies suggest that $InsP_3R$ activity affects APP processing, but pharmacological inhibition of γ-secretase is without effect on $InsP_3R$-mediated Ca^{2+} signaling (Oh and Turner, 2006). Thus, the γ-secretase activity of PS is likely not involved in this mechanism by which mutant PS regulates $InsP_3R$ channel gating.

The dependence of Aβ production on $InsP_3R$ expression observed here suggests that mutant PS-mediated exaggerated Ca^{2+} signaling could be a proximal mechanism in AD. Brain Aβ production is driven by neuronal activity (Cirrito et al., 2005; Kamenetz et al., 2003), suggesting that activity and metabolic patterns may contribute to Aβ production and amyloid deposition (Buckner et al., 2005). As-yet-unspecified activity- or metabolism-dependent mechanisms may cause preferential accumulation of amyloid that, over many years, may participate in AD pathology (Buckner et al., 2005). Because of a central role of Ca^{2+} in regulating both neuronal excitability (Verkhratsky, 2005) and cell metabolism (Balaban, 2002; McCormack et al., 1990), active brain regions are likely sites of higher Ca^{2+} signaling activity. Mutant PS-mediated exaggerated Ca^{2+} release activity of the $InsP_3R$ may therefore provide a mechanism for preferential accumulation of amyloid. Other mechanisms that do not involve either PS or $InsP_3R$, but that similarly cause chronic low-level exaggerated Ca^{2+} signaling might also be expected to result in AD pathology. Although speculative, such mechanisms could possibly be involved in sporadic forms of AD.

In summary, our results indicate that PS interact with the $InsP_3R$ Ca^{2+} release channel and modulate its gating activity. FAD mutant PS1 and PS2 exert stimulatory effects on $InsP_3R$ channel activity that result in perturbed cellular Ca^{2+} signaling. These data provide molecular insights into the mechanisms of enhanced $InsP_3$-mediated Ca^{2+} signals observed in cells that express FAD mutant presenilins, including those from AD patients. Enhanced Ca^{2+} release from the ER as a result of this interaction has physiological implications that may be relevant in AD, including enhanced APP processing. These observations may provide unique molecular insights into the "Ca^{2+} dysregulation hypothesis" of AD pathogenesis and suggest novel targets for therapeutic intervention.

EXPERIMENTAL PROCEDURES

Recombinant Baculovirus Constructs and Sf9 Cell Infection

Spodoptera frugiperda cells (Sf9, BD Biosciences) were maintained as described (Ionescu et al., 2006). Human PS baculovirus constructs (PS1-WT, PS1-M146L, PS2-WT, and PS2-N141I) were subcloned into pFastBac1; baculoviruses were generated using the Bac-to-Bac system (Invitrogen). Expression was confirmed by western blotting with anti-PS1 (monoclonal MAB5232, polyclonal MAB1563, Chemicon International, Inc.) and -PS2 (EMD Chemicals Inc.) antibodies. Localization of PS in Sf9 cells was confirmed by immunocytochemistry with anti-PS1 or -PS2 antibodies. Sf9 nuclei were counterstained with TOTO-3 nuclear dye (Molecular Probes).

Cell Culture and Transfection

DT40 cells were maintained as described (White et al., 2005). Human wild-type (WT) *PS1* and *M146L* cDNAs were subcloned into pIRES2-EGFP (Clontech). Cells were transfected using a Nucleofector Device (Amaxa). To select stable polyclonal lines, transfected cells were cultured for 2 weeks in 2 mg ml^{-1} Geneticin (Invitrogen). PS expression was confirmed by western blot. Human APP harboring Swedish mutations (APP_{SWE}) was introduced into PS1-expressing DT 40 lines by retrovirus infection. APP_{SWE} cDNA was subcloned into pΔMX-IRES-dsRED retrovirus vector. APP_{SWE} retrovirus was generated using Retro-X system (Clontech). Expression of APP_{SWE} was confirmed by western blotting using a polyclonal anti-APP antibody. Primary cortical neurons were prepared from embryonic day 15 (E15–16) C57BL/6J mice, as described (Meberg and Miller, 2003). Transfections were performed on 7- to 14-day-old cultures with pIRES2-EGFP-PS1WT, pIRES2-EGFP-M146L, or pIRES2-EGFP empty vector by n-Fect reagent (Neuromics). Experiments performed 48 hr after transfection.

Electrophysiology

Preparation of isolated nuclei from Sf9 or DT40 cells was as described (White et al., 2005). Nuclei were studied in standard bath solution: 140 mM KCl, 10 mM HEPES, and 0.5 mM BAPTA (free $[Ca^{2+}]$ = 300 nM) (pH 7.3). The pipette solution contained 140 mM KCl, 0.5 mM ATP, 10 mM HEPES, 1 μM free Ca^{2+} (pH 7.3). Free $[Ca^{2+}]$ in all solutions was adjusted, as described (Mak et al., 1998). Data were acquired at room temperature and analyzed as described (Ionescu et al., 2006).

Single-Cell Ca^{2+} Imaging

$[Ca^{2+}]_i$ was measured in Fura-2-loaded DT40 cells as described (White et al., 2005). ER Ca^{2+} content was estimated from changes in $[Ca^{2+}]_i$ in response to thapsigargin or ionomycin, as described (White et al., 2005), or with the low-affinity Ca^{2+} indicator Mag-Fura-2 (Invitrogen) following procedures similar to those described in Laude et al. (2005) modified for single-cell imaging. Following loading of cells on coverslips with Mag-Fura-2 (10 μM for 60 min), the plasma membranes were permeabilized by exposure to 10 μg/ml digitonin for 2 min in a medium that contained 220 nM Ca^{2+} and lacked MgATP. Following 30 min of continuous perfusion with the MgATP-free bath to wash out the digitonin, cells were alternately illuminated with 340/380 nm light and fluorescence intensity at 510 nm was collected with a Perkin Elmer Ultraview imaging system. Changes in $[Ca^{2+}]_{ER}$ are presented as changes in fluorescence ratio (R/R_0). R_0 was verified to reflect the ratio for Ca^{2+} depleted stores by using ionomycin (1 μM), as described (Laude et al., 2005). Ca^{2+} leak rates expressed as $\Delta(R/R_0)$ s^{-1}.

Amyloid Beta ($A\beta_{40}$ and $A\beta_{42}$) Determinations

Aβ levels in culture media were measured by sandwich ELISA (Suzuki et al., 1994). Briefly, plates were coated with Aβ N-terminal antibody Ban50 prior to application of cell media. The concentration of Aβ was determined using horseradish peroxidase (HRP)-conjugated BA27 or BC05 antibodies to detect $A\beta_{40}$ or $A\beta_{42}$, respectively. $A\beta_{40}$ or $A\beta_{42}$ levels were normalized to total protein concentration. Standard curves, constructed from serial dilutions of synthetic $A\beta_{40}$ or $A\beta_{42}$, were generated in each experiment.

Analysis and Statistics

Data were summarized as the mean ± SEM, and statistical significance of differences between means was assessed using unpaired t tests or analysis of variance (ANOVA) for repeated-measures at the 95% level ($p < 0.05$).

SUPPLEMENTAL DATA

The Supplemental Data for this article can be found online at http://www.neuron.org/cgi/content/full/58/6/871/DC1/.

ACKNOWLEDGMENTS

We thank Ikuo Hayashi for recombinant baculoviruses and Eric Swanson for help with neuron isolation. This work was supported by NIH GM56328 and MH059937 to J.K.F. and a Pilot Project from the Alzheimer's Disease Core Center at the University of Pennsylvania AG 10124.

Received: August 31, 2007
Revised: February 5, 2008
Accepted: April 16, 2008
Published: June 25, 2008

REFERENCES

Balaban, R.S. (2002). Cardiac energy metabolism homeostasis: role of cytosolic calcium. J. Mol. Cell. Cardiol. *34*, 1259–1271.

Barrow, P.A., Empson, R.M., Gladwell, S.J., Anderson, C.M., Killick, R., Yu, X., Jefferys, J.G., and Duff, K. (2000). Functional phenotype in transgenic mice expressing mutant human presenilin-1. Neurobiol. Dis. *7*, 119–126.

Berridge, M.J., Lipp, P., and Bootman, M.D. (2000). The versatility and universality of calcium signalling. Nat. Rev. Mol. Cell Biol. *1*, 11–21.

Blennow, K., de Leon, M.J., and Zetterberg, H. (2006). Alzheimer's disease. Lancet *368*, 387–403.

Buckner, R.L., Snyder, A.Z., Shannon, B.J., LaRossa, G., Sachs, R., Fotenos, A.F., Sheline, Y.I., Klunk, W.E., Mathis, C.A., Morris, J.C., and Mintun, M.A. (2005). Molecular, structural, and functional characterization of Alzheimer's disease: evidence for a relationship between default activity, amyloid, and memory. J. Neurosci. *25*, 7709–7717.

Buxbaum, J.D., Ruefli, A.A., Parker, C.A., Cypess, A.M., and Greengard, P. (1994). Calcium regulates processing of the Alzheimer amyloid protein precursor in a protein kinase C-independent manner. Proc. Natl. Acad. Sci. USA *91*, 4489–4493.

Cai, W., Hisatsune, C., Nakamura, K., Nakamura, T., Inoue, T., and Mikoshiba, K. (2004). Activity-dependent expression of inositol 1,4,5-trisphosphate receptor type 1 in hippocampal neurons. J. Biol. Chem. *279*, 23691–23698.

Cedazo-Minguez, A., Popescu, B.O., Ankarcrona, M., Nishimura, T., and Cowburn, R.F. (2002). The presenilin 1 deltaE9 mutation gives enhanced basal phospholipase C activity and a resultant increase in intracellular calcium concentrations. J. Biol. Chem. *277*, 36646–36655.

Chan, S.L., Mayne, M., Holden, C.P., Geiger, J.D., and Mattson, M.P. (2000). Presenilin-1 mutations increase levels of ryanodine receptors and calcium release in PC12 cells and cortical neurons. J. Biol. Chem. *275*, 18195–18200.

Cirrito, J.R., Yamada, K.A., Finn, M.B., Sloviter, R.S., Bales, K.R., May, P.C., Schoepp, D.D., Paul, S.M., Mennerick, S., and Holtzman, D.M. (2005). Synaptic activity regulates interstitial fluid amyloid-beta levels in vivo. Neuron *48*, 913–922.

Citron, M., Westaway, D., Xia, W., Carlson, G., Diehl, T., Levesque, G., Johnson-Wood, K., Lee, M., Seubert, P., Davis, A., et al. (1997). Mutant presenilins of Alzheimer's disease increase production of 42-residue amyloid beta-protein in both transfected cells and transgenic mice. Nat. Med. *3*, 67–72.

De Strooper, B. (2007). Loss-of-function presenilin mutations in Alzheimer disease. Talking point on the role of presenilin mutations in Alzheimer disease. EMBO Rep. *8*, 141–146.

Edbauer, D., Winkler, E., Regula, J.T., Pesold, B., Steiner, H., and Haass, C. (2003). Reconstitution of gamma-secretase activity. Nat. Cell Biol. *5*, 486–488.

Etcheberrigaray, R., Hirashima, N., Nee, L., Prince, J., Govoni, S., Racchi, M., Tanzi, R.E., and Alkon, D.L. (1998). Calcium responses in fibroblasts from asymptomatic members of Alzheimer's disease families. Neurobiol. Dis. *5*, 37–45.

Foskett, J.K., White, C., Cheung, K.H., and Mak, D.-O.D. (2007). Inositol trisphosphate receptor Ca^{2+} release channels. Physiol. Rev. *87*, 593–658.

Gandy, S., Doeven, M.K., and Poolman, B. (2006). Alzheimer disease: presenilin springs a leak. Nat. Med. *12*, 1121–1123.

Genazzani, A.A., Carafoli, E., and Guerini, D. (1999). Calcineurin controls inositol 1,4,5-trisphosphate type 1 receptor expression in neurons. Proc. Natl. Acad. Sci. USA *96*, 5797–5801.

Giacomello, M., Barbiero, L., Zatti, G., Squitti, R., Binetti, G., Pozzan, T., Fasolato, C., Ghidoni, R., and Pizzo, P. (2005). Reduction of Ca^{2+} stores and capacitative Ca^{2+} entry is associated with the familial Alzheimer's disease presenilin-2 T122R mutation and anticipates the onset of dementia. Neurobiol. Dis. *18*, 638–648.

Guo, Q., Furukawa, K., Sopher, B.L., Pham, D.G., Xie, J., Robinson, N., Martin, G.M., and Mattson, M.P. (1996). Alzheimer's PS-1 mutation perturbs calcium homeostasis and sensitizes PC12 cells to death induced by amyloid beta-peptide. Neuroreport *8*, 379–383.

Haass, C., and Selkoe, D.J. (2007). Soluble protein oligomers in neurodegeneration: lessons from the Alzheimer's amyloid beta-peptide. Nat. Rev. Mol. Cell Biol. *8*, 101–112.

Hardy, J. (2006). A hundred years of Alzheimer's disease research. Neuron *52*, 3–13.

Hardy, J., and Selkoe, D.J. (2002). The amyloid hypothesis of Alzheimer's disease: progress and problems on the road to therapeutics. Science *297*, 353–356.

Hebert, S.S., Serneels, L., Dejaegere, T., Horre, K., Dabrowski, M., Baert, V., Annaert, W., Hartmann, D., and De Strooper, B. (2004). Coordinated and widespread expression of gamma-secretase in vivo: evidence for size and molecular heterogeneity. Neurobiol. Dis. *17*, 260–272.

Hirashima, N., Etcheberrigaray, R., Bergamaschi, S., Racchi, M., Battaini, F., Binetti, G., Govoni, S., and Alkon, D.L. (1996). Calcium responses in human fibroblasts: a diagnostic molecular profile for Alzheimer's disease. Neurobiol. Aging *17*, 549–555.

Hutton, M., and Hardy, J. (1997). The presenilins and Alzheimer's disease. Hum. Mol. Genet. *6*, 1639–1646.

Ionescu, L., Cheung, K.H., Vais, H., Mak, D.O., White, C., and Foskett, J.K. (2006). Graded recruitment and inactivation of single $InsP_3$ receptor Ca^{2+}-release channels: implications for quantal Ca^{2+} release. J. Physiol. *573*, 645–662.

Ito, E., Oka, K., Etcheberrigaray, R., Nelson, T.J., McPhie, D.L., Tofel-Grehl, B., Gibson, G.E., and Alkon, D.L. (1994). Internal Ca^{2+} mobilization is altered in fibroblasts from patients with Alzheimer disease. Proc. Natl. Acad. Sci. USA *91*, 534–538.

Johnston, J.M., Burnett, P., Thomas, A.P., and Tezapsidis, N. (2006). Calcium oscillations in type-1 astrocytes, the effect of a presenilin 1 (PS1) mutation. Neurosci. Lett. *395*, 159–164.

Jolly-Tornetta, C., Gao, Z.Y., Lee, V.M., and Wolf, B.A. (1998). Regulation of amyloid precursor protein secretion by glutamate receptors in human Ntera 2 neurons. J. Biol. Chem. *273*, 14015–14021.

Kamenetz, F., Tomita, T., Hsieh, H., Seabrook, G., Borchelt, D., Iwatsubo, T., Sisodia, S., and Malinow, R. (2003). APP processing and synaptic function. Neuron *37*, 925–937.

Kasri, N.N., Kocks, S.L., Verbert, L., Hebert, S.S., Callewaert, G., Parys, J.B., Missiaen, L., and De Smedt, H. (2006). Up-regulation of inositol 1,4,5-trisphosphate receptor type 1 is responsible for a decreased endoplasmic-reticulum Ca^{2+} content in presenilin double knock-out cells. Cell Calcium *40*, 41–51.

LaFerla, F.M. (2002). Calcium dyshomeostasis and intracellular signalling in Alzheimer's disease. Nat. Rev. Neurosci. *3*, 862–872.

Laude, A.J., Tovey, S.C., Dedos, S.G., Potter, B.V., Lummis, S.C., and Taylor, C.W. (2005). Rapid functional assays of recombinant IP_3 receptors. Cell Calcium *38*, 45–51.

Leissring, M.A., Parker, I., and LaFerla, F.M. (1999a). Presenilin-2 mutations modulate amplitude and kinetics of inositol 1, 4,5-trisphosphate-mediated calcium signals. J. Biol. Chem. *274*, 32535–32538.

Leissring, M.A., Paul, B.A., Parker, I., Cotman, C.W., and LaFerla, F.M. (1999b). Alzheimer's presenilin-1 mutation potentiates inositol 1,4,5-trisphosphate-mediated calcium signaling in Xenopus oocytes. J. Neurochem. *72*, 1061–1068.

Leissring, M.A., Akbari, Y., Fanger, C.M., Cahalan, M.D., Mattson, M.P., and LaFerla, F.M. (2000). Capacitative calcium entry deficits and elevated luminal calcium content in mutant presenilin-1 knockin mice. J. Cell Biol. *149*, 793–798.

Leissring, M.A., LaFerla, F.M., Callamaras, N., and Parker, I. (2001). Subcellular mechanisms of presenilin-mediated enhancement of calcium signaling. Neurobiol. Dis. *8*, 469–478.

Lessard, C.B., Lussier, M.P., Cayouette, S., Bourque, G., and Boulay, G. (2005). The overexpression of presenilin2 and Alzheimer's-disease-linked presenilin2 variants influences TRPC6-enhanced Ca^{2+} entry into HEK293 cells. Cell. Signal. *17*, 437–445.

Mak, D.-O.D., McBride, S., and Foskett, J.K. (1998). Inositol 1,4,5-trisphosphate activation of inositol trisphosphate receptor Ca^{2+} channel by ligand tuning of Ca^{2+} inhibition. Proc. Natl. Acad. Sci. USA *95*, 15821–15825.

Mattson, M.P. (2004). Pathways towards and away from Alzheimer's disease. Nature *430*, 631–639.

Mattson, M.P., and Guo, Q. (1997). Cell and molecular neurobiology of presenilins: a role for the endoplasmic reticulum in the pathogenesis of Alzheimer's disease? J. Neurosci. Res. *50*, 505–513.

Mattson, M.P., and Chan, S.L. (2003). Neuronal and glial calcium signaling in Alzheimer's disease. Cell Calcium *34*, 385–397.

Mattson, M.P., Zhu, H., Yu, J., and Kindy, M.S. (2000). Presenilin-1 mutation increases neuronal vulnerability to focal ischemia in vivo and to hypoxia and glucose deprivation in cell culture: involvement of perturbed calcium homeostasis. J. Neurosci. *20*, 1358–1364.

McCormack, J.G., Halestrap, A.P., and Denton, R.M. (1990). Role of calcium ions in regulation of mammalian intramitochondrial metabolism. Physiol. Rev. *70*, 391–425.

Meberg, P.J., and Miller, M.W. (2003). Culturing hippocampal and cortical neurons. Methods Cell Biol. *71*, 111–127.

Nelson, O., Tu, H., Lei, T., Bentahir, M., de Strooper, B., and Bezprozvanny, I. (2007). Familial Alzheimer disease-linked mutations specifically disrupt Ca^{2+} leak function of presenilin 1. J. Clin. Invest. *117*, 1230–1239.

Oh, Y.S., and Turner, R.J. (2006). Effect of gamma-secretase inhibitors on muscarinic receptor-mediated calcium signaling in human salivary epithelial cells. Am. J. Physiol. Cell Physiol. *291*, C76–C82.

Querfurth, H.W., and Selkoe, D.J. (1994). Calcium ionophore increases amyloid beta peptide production by cultured cells. Biochemistry *33*, 4550–4561.

Scheuner, D., Eckman, C., Jensen, M., Song, X., Citron, M., Suzuki, N., Bird, T.D., Hardy, J., Hutton, M., Kukull, W., et al. (1996). Secreted amyloid beta-protein similar to that in the senile plaques of Alzheimer's disease is increased in vivo by the presenilin 1 and 2 and APP mutations linked to familial Alzheimer's disease. Nat. Med. *2*, 864–870.

Schneider, I., Reverse, D., Dewachter, I., Ris, L., Caluwaerts, N., Kuiperi, C., Gilis, M., Geerts, H., Kretzschmar, H., Godaux, E., et al. (2001). Mutant presenilins disturb neuronal calcium homeostasis in the brain of transgenic mice, decreasing the threshold for excitotoxicity and facilitating long-term potentiation. J. Biol. Chem. *276*, 11539–11544.

Shen, J., and Kelleher, R.J., 3rd. (2007). The presenilin hypothesis of Alzheimer's disease: evidence for a loss-of-function pathogenic mechanism. Proc. Natl. Acad. Sci. USA *104*, 403–409.

Smith, I.F., Boyle, J.P., Vaughan, P.F., Pearson, H.A., Cowburn, R.F., and Peers, C.S. (2002). Ca^{2+} stores and capacitative Ca^{2+} entry in human neuroblastoma (SH-SY5Y) cells expressing a familial Alzheimer's disease presenilin-1 mutation. Brain Res. *949*, 105–111.

Smith, I.F., Green, K.N., and LaFerla, F.M. (2005a). Calcium dysregulation in Alzheimer's disease: recent advances gained from genetically modified animals. Cell Calcium *38*, 427–437.

Smith, I.F., Hitt, B., Green, K.N., Oddo, S., and LaFerla, F.M. (2005b). Enhanced caffeine-induced Ca^{2+} release in the 3xTg-AD mouse model of Alzheimer's disease. J. Neurochem. *94*, 1711–1718.

Stutzmann, G.E. (2005). Calcium dysregulation, IP_3 signaling, and Alzheimer's disease. Neuroscientist *11*, 110–115.

Stutzmann, G.E., Caccamo, A., LaFerla, F.M., and Parker, I. (2004). Dysregulated IP3 signaling in cortical neurons of knock-in mice expressing an Alzheimer's-linked mutation in presenilin1 results in exaggerated Ca^{2+} signals and altered membrane excitability. J. Neurosci. *24*, 508–513.

Stutzmann, G.E., Smith, I., Caccamo, A., Oddo, S., Laferla, F.M., and Parker, I. (2006). Enhanced ryanodine receptor recruitment contributes to Ca^{2+} disruptions in young, adult, and aged Alzheimer's disease mice. J. Neurosci. *26*, 5180–5189.

Sugawara, H., Kurosaki, M., Takata, M., and Kurosaki, T. (1997). Genetic evidence for involvement of type 1, type 2 and type 3 inositol 1,4,5-trisphosphate receptors in signal transduction through the B-cell antigen receptor. EMBO J. *16*, 3078–3088.

Supnet, C., Grant, J., Kong, H., Westaway, D., and Mayne, M. (2006). Amyloid-beta-(1–42) increases ryanodine receptor-3 expression and function in neurons of TgCRND8 mice. J. Biol. Chem. *281*, 38440–38447.

Suzuki, N., Cheung, T.T., Cai, X.D., Odaka, A., Otvos, L., Jr., Eckman, C., Golde, T.E., and Younkin, S.G. (1994). An increased percentage of long amyloid beta protein secreted by familial amyloid beta protein precursor (beta APP717) mutants. Science *264*, 1336–1340.

Takeda, T., Asahi, M., Yamaguchi, O., Hikoso, S., Nakayama, H., Kusakari, Y., Kawai, M., Hongo, K., Higuchi, Y., Kashiwase, K., et al. (2005). Presenilin 2 regulates the systolic function of heart by modulating Ca^{2+} signaling. FASEB J. *19*, 2069–2071.

Tu, H., Nelson, O., Bezprozvanny, A., Wang, Z., Lee, S.F., Hao, Y.H., Serneels, L., De Strooper, B., Yu, G., and Bezprozvanny, I. (2006). Presenilins form ER Ca^{2+} leak channels, a function disrupted by familial Alzheimer's disease-linked mutations. Cell *126*, 981–993.

Verkhratsky, A. (2005). Physiology and pathophysiology of the calcium store in the endoplasmic reticulum of neurons. Physiol. Rev. *85*, 201–279.

White, C., Li, C., Yang, J., Petrenko, N.B., Madesh, M., Thompson, C.B., and Foskett, J.K. (2005). The endoplasmic reticulum gateway to apoptosis by Bcl-X_L modulation of the $InsP_3R$. Nat. Cell Biol. *7*, 1021–1028.

Yoo, A.S., Cheng, I., Chung, S., Grenfell, T.Z., Lee, H., Pack-Chung, E., Handler, M., Shen, J., Xia, W., Tesco, G., et al. (2000). Presenilin-mediated modulation of capacitative calcium entry. Neuron *27*, 561–572.

Zatti, G., Ghidoni, R., Barbiero, L., Binetti, G., Pozzan, T., Fasolato, C., and Pizzo, P. (2004). The presenilin 2 M239I mutation associated with familial Alzheimer's disease reduces Ca^{2+} release from intracellular stores. Neurobiol. Dis. *15*, 269–278.

Zatti, G., Burgo, A., Giacomello, M., Barbiero, L., Ghidoni, R., Sinigaglia, G., Florean, C., Bagnoli, S., Binetti, G., Sorbi, S., et al. (2006). Presenilin mutations linked to familial Alzheimer's disease reduce endoplasmic reticulum and Golgi apparatus calcium levels. Cell Calcium *39*, 539–550.

Naunyn-Schmiedeberg's Arch Pharmacol (2008) 377:295–300
DOI 10.1007/s00210-007-0206-2

REVIEW

At the frontline of Alzheimer's disease treatment: γ-secretase inhibitor/modulator mechanism

Taisuke Tomita

Received: 28 August 2007 / Accepted: 17 October 2007 / Published online: 24 November 2007

Abstract Genetic and biological studies provide evidence that the production and deposition of amyloid-β peptides (Aβ) contribute to the etiology of Alzheimer's disease. β- and γ-secretases, which are responsible for the generation of Aβ, are plausible molecular targets for Alzheimer's disease treatment. γ-Secretase is an unusual aspartic protease that cleaves the scissile bond within the transmembrane domain. This unusual enzyme is composed of a high molecular weight membrane protein complex containing presenilin, nicastrin, Aph-1 and Pen-2. Drugs that regulate the production of Aβ by inhibiting or modulating γ-secretase activity could provide a disease-modifying effect on Alzheimer's disease, although recent studies suggest that γ-secretase plays important roles in cellular signaling including Notch. Thus, understanding the molecular mechanism whereby γ-secretase recognizes and cleaves its substrate is a critical issue for the development of compounds that specifically regulate Aβ-generating γ-secretase activity. This review focuses on the structure and function relationship of γ-secretase complex and the mode of action of the γ-secretase inhibitors.

Keywords Alzheimer's disease · Secretase · Amyloid-β peptide · Intramembrane proteolysis · Protease

T. Tomita (✉)
Department of Neuropathology and Neuroscience, Graduate School of Pharmaceutical Sciences, The University of Tokyo,
7-3-1 Hongo, Bunkyo-ku,
Tokyo 113-0033, Japan
e-mail: taisuke@mol.f.u-tokyo.ac.jp

Introduction

Alzheimer's disease (AD) is a progressive dementing neurodegenerative disorder in the elderly characterized pathologically by the presence of senile plaques and neurofibrillary changes in the brains of affected individuals. Senile plaques are composed of amyloid-β peptides (Aβ) that are proteolytically produced from amyloid-β precursor protein (APP). APP is initially cleaved by β-secretase to generate a 99-residue C-terminal fragment (C99) that is subsequently cleaved by γ-secretase to generate Aβ (Fig. 1). C-terminal length of Aβ generated by γ-secretase is heterogeneous; Aβ42 is relatively a minor molecular species of the Aβ secreted from cells. However, Aβ42 is the initially and predominantly deposited Aβ species in AD brains, and aggregates much faster than the predominant Aβ40 species (Iwatsubo et al. 1994). Genetic mutations in presenilin 1 (PS1) and PS2 genes were found to cause familial AD (FAD) associated with an increase in Aβ42 production (Borchelt et al. 1996; Tomita et al. 1997). In contrast, ablation of PS genes abolished the γ-secretase activity (De Strooper et al. 1998; Herreman et al. 2000). These data implicated a seminal role of the generation and production of Aβ42 by γ-secretase activity, that is regulated by PS, in the pathogenesis of AD (Tomita and Iwatsubo 2006).

Functional characterization of γ-secretase complex

γ-Secretase is an unusual protease that cleaves the scissile bond within the transmembrane domain (TMD) of APP (Tomita and Iwatsubo 2006; Wolfe 2006). Extensive analyses revealed that γ-secretase is composed of a high molecular weight membrane protein complex containing PS, nicastrin (Nct), Aph-1 and Pen-2 (Fig. 2) (Takasugi et al. 2003). PS is

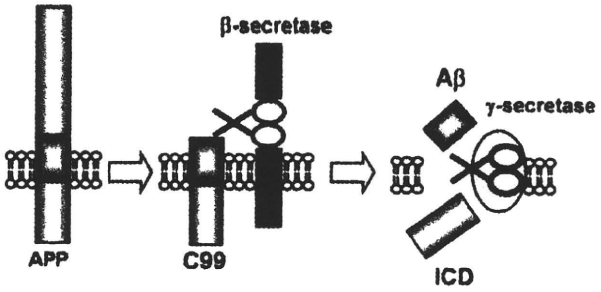

Fig. 1 Proteolytic processing of APP. APP is first shed by β-secretase in luminal side to generate C99, which is a direct substrate for γ-secretase. γ-Secretase cleavage occurs within transmembrane region to release Aβ and the intracellular domain (ICD)

a highly conserved, polytopic integral membrane protein that spans membrane nine times and undergoes endoproteolysis to generate NH_2- and COOH-terminal fragments (NTF and CTF, respectively) (Thinakaran et al. 1996). Nct, identified by immunoisolation of PS complex, is a type-1 transmembrane protein that harbors a large glycosylated ectodomain (Yu et al. 2000). Finally, genetic studies in *Caenorhabditis elegans* and *Drosophila melanogaster* have revealed two additional polytopic membrane proteins, Aph-1 and Pen-2 (Goutte et al. 2002; Francis et al. 2002).

All four components are required for γ-secretase activity; genetic ablation or RNAi knockdown of one or the other of the components caused the loss of γ-secretase activity. Moreover, overexpression of any combination of the three proteins had no effect on γ-secretase activity, whereas overexpression of all four proteins caused the full assembly of γ-secretase complex and the reconstitution of proteolytic activity (Edbauer et al. 2003; Takasugi et al. 2003; Hayashi et al. 2004). Thus, these four proteins are necessary and sufficient for proteolytic activity, and membrane protein complex consisting of these proteins appears to be the minimal set of γ-secretase complex.

Through genetic studies using model animals such as nematodes and flies, it became clear that Notch signaling is mediated by the liberation of the Notch intracellular domain (NICD) from the membrane-tethered precursor by γ-secretase (Ilagan and Kopan 2007). NICD traverses to the nucleus where it is involved in gene transcription, which regulates the developmental and differentiation program in several cells and organs. Moreover, additional substrates for γ-secretase-mediated intramembrane proteolysis have now been identified. Like NICD, many of the substrate-derived intracellular domains (ICDs) are predicted to translocate into nucleus and mediate transcriptional regulation (Kopan and Ilagan 2004). Thus, γ-secretase mediates the intramembrane cleavages of type I transmembrane proteins to liberate ICDs, and in some case it might regulate nuclear signaling.

Several molecular, cellular, and chemical biological approaches have revealed the function of γ-secretase components in the intramembrane proteolysis (Tomita and Iwatsubo 2006). Highly conserved two aspartates within TMD6 and TMD7 were obligatory for the γ-secretase activity (Wolfe et al. 1999). Furthermore, the solubilized γ-secretase activity was fractionated together with PS fragments, and transition-state analog-type γ-secretase inhibitors covalently labeled PS fragments (Li et al. 2000a,b). These studies suggest that PS fragments might serve as the active center of γ-secretase. Moreover, recently, it was revealed that the ectodomain of Nct recognizes the N terminus of γ-secretase substrates, which is exposed after shedding (Shah et al. 2005). Thus, Nct can be considered a primary substrate binding site ("exosite") for the γ-secretase complex.

In contrast, the precise function of Aph-1 and Pen-2 has been obscure. Aph-1 is implicated in the assembly of γ-secretase complex as a scaffold protein (Niimura et al. 2005), and Pen-2 is required for the activation of enzymatic complex in the final step of the assembly. Recently, we found that the N terminus of Pen-2 regulates the cleavage of γ-secretase complex (Isoo et al. 2007). In addition, recent protein chemical approaches revealed the novel γ-

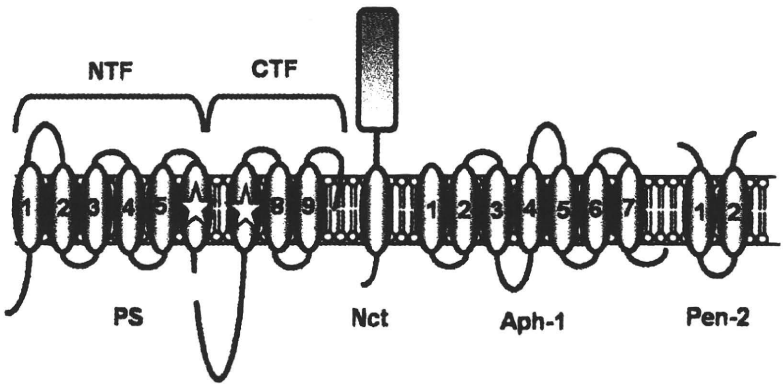

Fig. 2 Components of the γ-secretase complex. γ-Secretase is composed of four different integral membrane proteins; PS, Nct, Aph-1, and Pen-2. Presenilin undergoes endoproteolysis to generate NTF and CTF that remain associated. Two conserved aspartates (depicted by *stars*) within adjacent transmembrane domains are essential for both presenilin endoproteolysis and γ-secretase activity

secretase components that affect the proteolytic activity (i.e., CD147, TMP21) (Zhou et al. 2005; Chen et al. 2006). These proteins were dispensable for but modulated the proteolytic activity. It may be possible that γ-secretase complex is able to exchange several auxiliary subunits to modulate its activity and/or subcellular localization to cleave a variety of substrates in a similar fashion to that of proteasome. Focused proteomics approach would enable to uncover the whole picture of γ-secretase complex (Parks and Curtis 2007).

To understand the mechanism of the intramembrane proteolysis, structural analyses of γ-secretase complex would be required. However, the hydrophobic nature of γ-secretase made conventional approaches (e.g., X-ray crystallography, nuclear magnetic resonance [NMR]) difficult. To understand the structure of γ-secretase in functional state, we and others recently performed substituted cysteine accessibility method (SCAM) (Sato et al. 2006; Tolia et al. 2006). SCAM is a biochemistry-based structural analysis to identify the protein topology and the domain that is involved in the formation of hydrophilic pore or channel within the lipid bilayer. We applied SCAM for PS molecule, that is the catalytic subunit for proteolytic activity within the membrane.

We found that some cysteines introduced into TMD6 and TMD7 that harbor the two catalytic aspartates were labeled by MTSEA-biotin that is a membrane-impermeant, aqueous, and thiol-specific reagent, indicating that TMD6 and TMD7 contribute to the formation of a hydrophilic catalytic pore within the membrane. Moreover, recently, we and others reported the total structure of γ-secretase complex using electron microscopic observation and single particle analysis (Ogura et al. 2006; Lazarov et al. 2006). Importantly, the pore-like structure was identified within putative membrane-embedded region, while the resolution of this approach is still low (Steiner et al. 2006). Further attempts to understand the structure and the function of γ-secretase would be required for the understanding of the molecular mechanism of this unusual enzymatic reaction.

Mode of action of γ-secretase inhibitors and modulators

To date, several γ-secretase inhibitors have been reported (Fig. 3) (Tomita and Iwatsubo 2006; Schmidt et al. 2006). They block the cleavage of APP and other substrates, including Notch. In fact, acute administration of potent γ-secretase inhibitors to APP transgenic mice reduced Aβ levels in brain, but caused gastrointestinal toxicity in rats due to disruption of Notch signaling in the ileum (Searfoss et al. 2003). In view of the adverse effects caused by blockade of Notch signaling, there is a compelling need for the identification of the "therapeutic window" for avoiding the adverse effect, and the development of selective inhibitors that can inhibit only Aβ generation. In fact, LY450139, the derivative of dipeptidic γ-secretase inhibitor, which inhibited Notch signaling *in vitro*, was administered to human subjects and reduced Aβ levels without apparent Notch-based adverse effect (Siemers et al. 2005, 2006). LY450139 is claimed to be mildly selective for γ-secretase cleavage over the Notch signaling *in vivo*.

Several pharmaceutical companies published the patents regarding compounds containing sulfonamide or sulfone moiety as γ-secretase inhibitors. Some derivatives showed selective inhibitory effect on APP-cleaving γ-secretase activity, while the mode of action of these compounds has not been reported yet (Barten et al. 2005). Moreover, chloroisocoumarin derivatives and certain kinase inhibitors also inhibited Aβ production without affecting Notch cleavage in a cell-based assay (Petit et al. 2001; Netzer et al. 2003). In addition, it has recently been shown that a subset of NSAIDs and related derivatives selectively

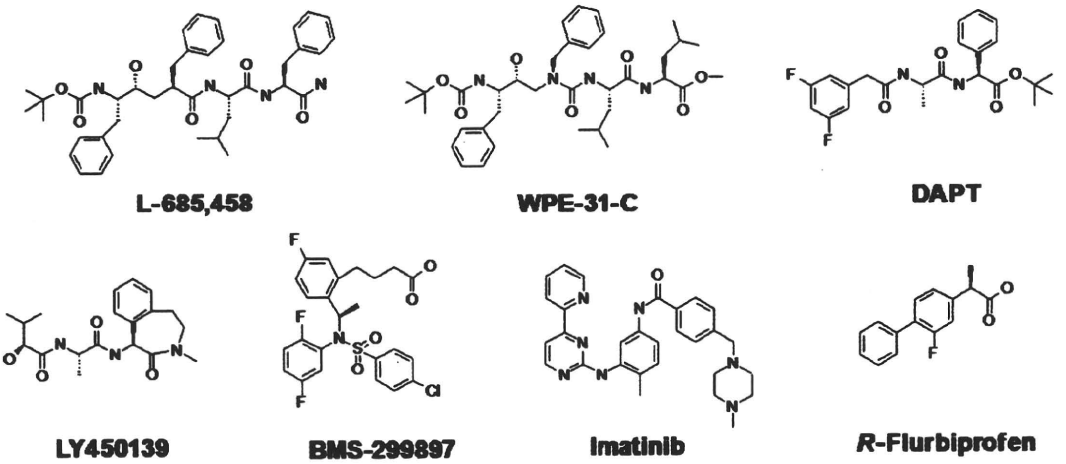

Fig. 3 γ-Secretase inhibitors. These include transition-state analogs (L-685,458, WPE-III-31C), dipeptidic inhibitors (DAPT, LY450139), sulfonamide (BMS-299897), kinase inhibitor (imatinib) and NSAIDs (*R*-Flurbiprofen)

decreased the secretion of aggregable Aβ42 *in vitro* and *in vivo* without affecting the total Aβ levels (Weggen et al. 2001; Takahashi et al. 2003). Importantly, this class of compounds also affected the cleavage sites by γ-secretase in Notch without apparent inhibition of Notch signaling, suggesting that these compounds modulate only the scissile bond position within TMD of the substrate (Okochi et al. 2006). Thus, it may be possible to avoid the envisaged adverse effects of γ-secretase inhibition by developing Notch-sparing γ-secretase inhibitors and γ-secretase modulators.

Elucidation of the mechanism by which these γ-secretase inhibitors and modulators regulate γ-secretase activity awaits further investigation. Recently, however, chemical biological approach is emerging for the understanding of the mode of action of inhibitors. In fact, the affinity-based labeling and isolation experiments using transition-state inhibitors revealed that PS complex represents the long-sought γ-secretase (Li et al. 2000b; Esler et al. 2000). We recently developed the novel γ-secretase inhibitor-based chemical probes that carry photoaffinity (i.e., benzophenone) and biotin moieties for crosslinking and purification, respectively (Morohashi et al. 2006; Fuwa et al. 2007). These photoprobes enable us to directly identify the molecular target of the small compounds by irradiation experiment.

Using this technique, we unequivocally identified that dipeptidic inhibitors such as DAPT, compound E and DBZ targeted directly to PS fragments, the catalytic subunit of γ-secretase. Importantly, DAPT, the γ-secretase specific inhibitor, bound to PS CTF, while compound E and DBZ that have cross-inhibitory potency against other family protease (i.e., signal peptide peptidase) targeted to PS NTF. These results provide molecular information of the specificity of γ-secretase inhibitors. Identification of the molecular target of the sulfonamide-based Notch-sparing γ-secretase inhibitor is currently underway (Fuwa et al. 2006). Moreover, structural analyses using fluorescence resonance energy transfer and SCAM identified that γ-secretase modulators caused conformational changes in PS polypeptides (Lleo et al. 2004; Isoo et al. 2007), suggesting that the structural modulation of the γ-secretase is the target molecular mechanism for therapeutic intervention. Further attempts to define the molecular mechanism of the compounds and to screen its derivatives specifically relevant to APP cleavage will facilitate not only development of novel therapeutic drug for AD, but also understanding of the unusual intramembrane proteolytic activity.

Conclusion

During the past two decades, the molecular details for the pathogenesis of AD have become clear enough to enable us to develop therapeutic strategies. Genetic and biochemical studies strongly implicate Aβ as a key molecule in the etiology of AD, suggesting that interfering with the production of Aβ could be a promising therapeutic strategy. γ-Secretase is an unusual enzyme that cleaves scissile bond within TMD and one of the plausible molecular targets for AD treatment. Moreover, discovery of several γ-secretase inhibitors and application for biological studies dramatically enhanced our understanding of the enzymatic characteristics of γ-secretase. Selective inhibition of APP cleavage remains to be a critical issue because γ-secretase activity is important for other signaling events. Nonetheless, certain compounds that specifically reduce APP cleavage are recently emerging. Further extensive efforts in both academic and pharmaceutical laboratories may raise high hopes for the promising therapeutics for AD.

Acknowledgments I am grateful to Dr. Takeshi Iwatsubo (The University of Tokyo) and all colleagues who collaborated in the studies cited in this review.

References

Barten DM, Guss VL, Corsa JA, Loo A, Hansel SB, Zheng M, Munoz B, Srinivasan K, Wang B, Robertson BJ, Polson CT, Wang J, Roberts SB, Hendrick JP, Anderson JJ, Loy JK, Denton R, Verdoorn TA, Smith DW, Felsenstein KM (2005) Dynamics of β-amyloid reductions in brain, cerebrospinal fluid, and plasma of β-amyloid precursor protein transgenic mice treated with a γ-secretase inhibitor. J Pharmacol Exp Ther 312:635–643

Borchelt DR, Thinakaran G, Eckman CB, Lee MK, Davenport F, Ratovitsky T, Prada CM, Kim G, Seekins S, Yager D, Slunt HH, Wang R, Seeger M, Levey AI, Gandy SE, Copeland NG, Jenkins NA, Price DL, Younkin SG, Sisodia SS (1996) Familial Alzheimer's disease-linked presenilin 1 variants elevate Aβ1-42/1-40 ratio *in vitro* and *in vivo*. Neuron 17:1005–1013

Chen F, Hasegawa H, Schmitt-Ulms G, Kawarai T, Bohm C, Katayama T, Gu Y, Sanjo N, Glista M, Rogaeva E, Wakutani Y, Pardossi-Piquard R, Ruan X, Tandon A, Checler F, Marambaud P, Hansen K, Westaway D, St George-Hyslop P, Fraser P (2006) TMP21 is a presenilin complex component that modulates γ-secretase but not ε-secretase activity. Nature 440:1208–1212

De Strooper B, Saftig P, Craessaerts K, Vanderstichele H, Guhde G, Annaert W, Von Figura K, Van Leuven F (1998) Deficiency of presenilin-1 inhibits the normal cleavage of amyloid precursor protein. Nature 391:387–390

Edbauer D, Winkler E, Regula JT, Pesold B, Steiner H, Haass C (2003) Reconstitution of γ-secretase activity. Nat Cell Biol 5:486–488

Esler WP, Kimberly WT, Ostaszewski BL, Diehl TS, Moore CL, Tsai JY, Rahmati T, Xia W, Selkoe DJ, Wolfe MS (2000) Transition-state analogue inhibitors of γ-secretase bind directly to presenilin-1. Nat Cell Biol 2:428–434

Francis R, McGrath G, Zhang J, Ruddy DA, Sym M, Apfeld J, Nicoll M, Maxwell M, Hai B, Ellis MC, Parks AL, Xu W, Li J, Gurney M, Myers RL, Himes CS, Hiebsch R, Ruble C, Nye JS, Curtis D (2002) *aph-1* and *pen-2* are required for Notch pathway signaling, γ-secretase cleavage of βAPP, and presenilin protein accumulation. Dev Cell 3:85–97

Fuwa H, Hiromoto K, Takahashi Y, Yokoshima S, Kan T, Fukuyama T, Iwatsubo T, Tomita T, Natsugari H (2006) Synthesis of biotinylated photoaffinity probes based on arylsulfonamide γ-secretase inhibitors. Bioorg Med Chem Lett 16:4184–4189

Fuwa H, Takahashi Y, Konno Y, Watanabe N, Miyashita H, Sasaki M, Natsugari H, Kan T, Fukuyama T, Tomita T, Iwatsubo T (2007) Divergent synthesis of multifunctional molecular probes to elucidate the enzyme specificity of dipeptidic γ-secretase inhibitors. ACS Chem Biol 2:408–418

Goutte C, Tsunozaki M, Hale VA, Priess JR (2002) APH-1 is a multipass membrane protein essential for the Notch signaling pathway in *Caenorhabditis elegans* embryos. Proc Natl Acad Sci USA 99:775–779

Hayashi I, Urano Y, Fukuda R, Isoo N, Kodama T, Hamakubo T, Tomita T, Iwatsubo T (2004) Selective reconstitution and recovery of functional γ-secretase complex on budded baculovirus particles. J Biol Chem 279:38040–38046

Herreman A, Serneels L, Annaert W, Collen D, Schoonjans L, De Strooper B (2000) Total inactivation of γ-secretase activity in presenilin-deficient embryonic stem cells. Nat Cell Biol 2: 461–462

Ilagan MX, Kopan R (2007) SnapShot: notch signaling pathway. Cell 128:1246

Isoo N, Sato C, Miyashita H, Shinohara M, Takasugi N, Morohashi Y, Tsuji S, Tomita T, Iwatsubo T (2007) Aβ42 overproduction associated with structural changes in the catalytic pore of γ-secretase: common effects of Pen-2 N-terminal elongation and fenofibrate. J Biol Chem 282:12388–12396

Iwatsubo T, Odaka A, Suzuki N, Mizusawa H, Nukina N, Ihara Y (1994) Visualization of Aβ 42(43) and Aβ 40 in senile plaques with end-specific Aβ monoclonals: evidence that an initially deposited species is Aβ 42(43). Neuron 13:45–53

Kopan R, Ilagan MX (2004) γ-Secretase: proteasome of the membrane? Nat Rev Mol Cell Biol 5:499–504

Lazarov VK, Fraering PC, Ye W, Wolfe MS, Selkoe DJ, Li H (2006) Electron microscopic structure of purified, active γ-secretase reveals an aqueous intramembrane chamber and two pores. Proc Natl Acad Sci USA 103:6889–6894

Li YM, Lai MT, Xu M, Huang Q, DiMuzio-Mower J, Sardana MK, Shi XP, Yin KC, Shafer JA, Gardell SJ (2000a) Presenilin 1 is linked with γ-secretase activity in the detergent solubilized state. Proc Natl Acad Sci USA 97:6138–6143

Li YM, Xu M, Lai MT, Huang Q, Castro JL, DiMuzio-Mower J, Harrison T, Lellis C, Nadin A, Neduvelil JG, Register RB, Sardana MK, Shearman MS, Smith AL, Shi XP, Yin KC, Shafer JA, Gardell SJ (2000b) Photoactivated γ-secretase inhibitors directed to the active site covalently label presenilin 1. Nature 405:689–694

Lleo A, Berezovska O, Herl L, Raju S, Deng A, Bacskai BJ, Frosch MP, Irizarry M, Hyman BT (2004) Nonsteroidal anti-inflammatory drugs lower Aβ42 and change presenilin 1 conformation. Nat Med 10:1065–1066

Morohashi Y, Kan T, Tominari Y, Fuwa H, Okamura Y, Watanabe N, Sato C, Natsugari H, Fukuyama T, Iwatsubo T, Tomita T (2006) C-terminal fragment of presenilin is the molecular target of a dipeptidic γ-secretase-specific inhibitor DAPT. J Biol Chem 281:14670–14676

Netzer WJ, Dou F, Cai D, Veach D, Jean S, Li Y, Bornmann WG, Clarkson B, Xu H, Greengard P (2003) Gleevec inhibits β-amyloid production but not Notch cleavage. Proc Natl Acad Sci USA 100:12444–12449

Niimura M, Isoo N, Takasugi N, Tsuruoka M, Ui-Tei K, Saigo K, Morohashi Y, Tomita T, Iwatsubo T (2005) Aph-1 contributes to the stabilization and trafficking of the γ-secretase complex through mechanisms involving intermolecular and intramolecular interactions. J Biol Chem 280:12967–12975

Ogura T, Mio K, Hayashi I, Miyashita H, Fukuda R, Kopan R, Kodama T, Hamakubo T, Iwatsubo T, Tomita T, Sato C (2006) Three-dimensional structure of the γ-secretase complex. Biochem Biophys Res Commun 343:525–534

Okochi M, Fukumori A, Jiang J, Itoh N, Kimura R, Steiner H, Haass C, Tagami S, Takeda M (2006) Secretion of the Notch-1 Aβ-like peptide during Notch signaling. J Biol Chem 281:7890–7898

Parks AL, Curtis D (2007) Presenilin diversifies its portfolio. Trends Genet 23:140–150

Petit A, Bihel F, Alves da Costa C, Pourquie O, Checler F, Kraus JL (2001) New protease inhibitors prevent γ-secretase-mediated production of Aβ40/42 without affecting Notch cleavage. Nat Cell Biol 3:507–511

Sato C, Morohashi Y, Tomita T, Iwatsubo T (2006) Structure of the catalytic pore of γ-secretase probed by the accessibility of substituted cysteines. J Neurosci 26:12081–12088

Schmidt B, Baumann S, Braun HA, Larbig G (2006) Inhibitors and modulators of β- and γ-secretase. Curr Top Med Chem 6:377–392

Searfoss GH, Jordan WH, Calligaro DO, Galbreath EJ, Schirtzinger LM, Berridge BR, Gao H, Higgins MA, May PC, Ryan TP (2003) Adipsin, a biomarker of gastrointestinal toxicity mediated by a functional γ-secretase inhibitor. J Biol Chem 278:46107–46116

Shah S, Lee SF, Tabuchi K, Hao YH, Yu C, LaPlant Q, Ball H, Dann CE 3rd, Sudhof T, Yu G (2005) Nicastrin functions as a γ-secretase-substrate receptor. Cell 122:435–447

Siemers E, Skinner M, Dean RA, Gonzales C, Satterwhite J, Farlow M, Ness D, May PC (2005) Safety, tolerability, and changes in amyloid β concentrations after administration of a γ-secretase inhibitor in volunteers. Clin Neuropharmacol 28:126–132

Siemers ER, Quinn JF, Kaye J, Farlow MR, Porsteinsson A, Tariot P, Zoulnouni P, Galvin JE, Holtzman DM, Knopman DS, Satterwhite J, Gonzales C, Dean RA, May PC (2006) Effects of a γ-secretase inhibitor in a randomized study of patients with Alzheimer disease. Neurology 66:602–604

Steiner H, Than M, Bode W, Haass C (2006) Pore-forming scissors? A first structural glimpse of γ-secretase. Trends Biochem Sci 31:491–493

Takahashi Y, Hayashi I, Tominari Y, Rikimaru K, Morohashi Y, Kan T, Natsugari H, Fukuyama T, Tomita T, Iwatsubo T (2003) Sulindac sulfide is a noncompetitive γ-secretase inhibitor that preferentially reduces Aβ42 generation. J Biol Chem 278:18664–18670

Takasugi N, Tomita T, Hayashi I, Tsuruoka M, Niimura M, Takahashi Y, Thinakaran G, Iwatsubo T (2003) The role of presenilin cofactors in the γ-secretase complex. Nature 422:438–441

Thinakaran G, Borchelt DR, Lee MK, Slunt HH, Spitzer L, Kim G, Ratovitsky T, Davenport F, Nordstedt C, Seeger M, Hardy J, Levey AI, Gandy SE, Jenkins NA, Copeland NG, Price DL, Sisodia SS (1996) Endoproteolysis of presenilin 1 and accumulation of processed derivatives *in vivo*. Neuron 17:181–190

Tolia A, Chavez-Gutierrez L, De Strooper B (2006) Contribution of presenilin transmembrane domains 6 and 7 to a water-containing cavity in the γ-secretase complex. J Biol Chem 281:27633–27642

Tomita T, Iwatsubo T (2006) γ-Secretase as a therapeutic target for treatment of Alzheimer's disease. Curr Pharm Des 12:661–670

Tomita T, Maruyama K, Saido TC, Kume H, Shinozaki K, Tokuhiro S, Capell A, Walter J, Grunberg J, Haass C, Iwatsubo T, Obata K (1997) The presenilin 2 mutation (N141I) linked to familial Alzheimer disease (Volga German families) increases the secretion of amyloid β protein ending at the 42nd (or 43rd) residue. Proc Natl Acad Sci USA 94:2025–2030

Weggen S, Eriksen JL, Das P, Sagi SA, Wang R, Pietrzik CU, Findlay KA, Smith TE, Murphy MP, Bulter T, Kang DE, Marquez-Sterling N, Golde TE, Koo EH (2001) A subset of NSAIDs lower amyloidogenic Aβ42 independently of cyclooxygenase activity. Nature 414:212–216

Wolfe MS (2006) The γ-Secretase complex: membrane-embedded proteolytic ensemble. Biochemistry 45:7931–7939

Wolfe MS, Xia W, Ostaszewski BL, Diehl TS, Kimberly WT, Selkoe DJ (1999) Two transmembrane aspartates in presenilin-1 required for presenilin endoproteolysis and γ-secretase activity. Nature 398:513–517

Yu G, Nishimura M, Arawaka S, Levitan D, Zhang L, Tandon A, Song YQ, Rogaeva E, Chen F, Kawarai T, Supala A, Levesque L, Yu H, Yang DS, Holmes E, Milman P, Liang Y, Zhang DM, Xu DH, Sato C, Rogaev E, Smith M, Janus C, Zhang Y, Aebersold R, Farrer LS, Sorbi S, Bruni A, Fraser P, St George-Hyslop P (2000) Nicastrin modulates presenilin-mediated notch/glp-1 signal transduction and βAPP processing. Nature 407:48–54

Zhou S, Zhou H, Walian PJ, Jap BK (2005) CD147 is a regulatory subunit of the γ-secretase complex in Alzheimer's disease amyloid β-peptide production. Proc Natl Acad Sci USA 102:7499–7504

Neurobiology of Disease

The C-Terminal PAL Motif and Transmembrane Domain 9 of Presenilin 1 Are Involved in the Formation of the Catalytic Pore of the γ-Secretase

Chihiro Sato,[1,2,3] Shizuka Takagi,[1] Taisuke Tomita,[1,3] and Takeshi Iwatsubo[1,2,3]

[1]Department of Neuropathology and Neuroscience, Graduate School of Pharmaceutical Sciences, and [2]Department of Neuropathology, Graduate School of Medicine, The University of Tokyo, and [3]Core Research for Evolutional Science and Technology, Japan Science and Technology Corporation, Bunkyo, Tokyo 113-0033, Japan

γ-Secretase is an unusual membrane-embedded protease, which cleaves the transmembrane domains (TMDs) of type I membrane proteins, including amyloid-β precursor protein and Notch receptor. We have previously shown the existence of a hydrophilic pore formed by TMD6 and TMD7 of presenilin 1 (PS1), the catalytic subunit of γ-secretase, within the membrane by the substituted cysteine accessibility method. Here we analyzed the structure of TMD8, TMD9, and the C terminus of PS1, which encompass the conserved PAL motif and the hydrophobic C-terminal tip, both being critical for the catalytic activity and the formation of the γ-secretase complex. We found that the amino acid residues around the PAL motif and the extracellular/luminal portion of TMD9 are highly water accessible and located in proximity to the catalytic pore. Furthermore, the region starting from the luminal end of TMD9 toward the C terminus forms an amphipathic α-helix-like structure that extends along the interface between the membrane and the extracellular milieu. Competition analysis using γ-secretase inhibitors revealed that the TMD9 is involved in the initial binding of substrates, as well as in the subsequent catalytic process as a subsite. Our results provide mechanistic insights into the role of TMD9 in the formation of the catalytic pore and the substrate entry, crucial to the unusual mode of intramembrane proteolysis by γ-secretase.

Key words: **Alzheimer's disease; amyloid beta; intramembrane-cleaving protease; presenilin; secretase; substituted cysteine accessibility method; Aβ peptide; structure**

Introduction

Intramembrane-cleaving proteases (I-CLiPs) are a family of polytopic membrane-embedded enzymes responsible for hydrolyzing substrates within the hydrophobic transmembrane domains (TMDs) (Wolfe and Kopan, 2004). Various I-CLiPs have so far been identified, including site 2 protease (S2P), signal peptide peptidase (SPP), rhomboid, and γ-secretase. γ-Secretase is an atypical aspartic protease that cleaves a set of type-1 single-span membrane proteins including amyloid precursor protein to form amyloid-β (Aβ) peptides in Alzheimer's disease (Tomita and Iwatsubo, 2006; Selkoe and Wolfe, 2007). γ-Secretase requires the formation of multimeric membrane protein complex comprised of nicastrin, Aph-1, and Pen-2 in addition to PS1 to exert the proteolytic activity (Takasugi et al., 2003), which hampered the conventional structural analysis, such as x-ray crystallography. Recently, a glimpse into the whole structure of the γ-secretase complex was obtained by single particle analysis (Lazarov et al., 2006; Ogura et al., 2006). However, because of the low resolution, these structures have not been helpful in deciphering the molecular mechanism of intramembrane proteolysis by γ-secretase. We have adopted the substituted cysteine accessibility method (SCAM) to analyze the structure of PS1. SCAM has been used to obtain structural information about various multipass membrane proteins, by forming covalent modification of sulfhydryl reagents to substituted cysteine (Cys) residues (Karlin and Akabas, 1998; Kaback et al., 2001). Using SCAM, we and others have shown that TMD6 and TMD7 of PS1 constitute the hydrophilic catalytic pore within membrane, and that the structural change of the pore correlates to the cleavage specificity (Sato et al., 2006; Tolia et al., 2006; Isoo et al., 2007). The recent x-ray crystallographic analyses of rhomboid and S2P revealed that their active sites reside in a water-filled "cavity" within the lipid bilayer (Y. Wang et al., 2006; Wu et al., 2006; Feng et al., 2007), suggesting that the hydrophilic active site located in the lipid bilayer is a structure common to I-CLiPs. Considering that the substrates for I-CLiPs also are embedded within the membrane, they should

Received March 18, 2008; revised April 23, 2008; accepted May 12, 2008.

This work was supported by grants-in-aid from the Ministry of Education, Culture, Sports, Science, and Technology of Japan (C.S., T.T., T.I.), by the Program for Promotion of Fundamental Studies in Health Sciences of the National Institute of Biomedical Innovation (T.T., T.I.), by Targeted Proteins Research Program of the Japan Science and Technology Corporation (JST) (T.T., T.I.), and by Core Research for Evolutional Science and Technology of JST (C.S., T.T., T.I.), Japan. We thank Drs. G. Thinakaran (University of Chicago, Chicago, IL), A. Takashima (RIKEN, Wako, Saitama, Japan), and H. Saya (Keio University, Shinjuku, Tokyo, Japan) for antibodies, B. De Strooper (Katholieke Universiteit Leuven, Leuven, The Netherlands) for DKO cells, T. Kitamura (The University of Tokyo, Minato, Tokyo, Japan) for retroviral infection system, and Takeda Pharmaceutical Company for Aβ ELISA. We are also grateful to our lab members for helpful discussions and technical assistance.

Correspondence should be addressed to Dr. Taisuke Tomita, Department of Neuropathology and Neuroscience, Graduate School of Pharmaceutical Sciences, The University of Tokyo, 7-3-1 Hongo, Bunkyo-ku, Tokyo 113-0033, Japan. E-mail: taisuke@mol.f.u-tokyo.ac.jp.

DOI:10.1523/JNEUROSCI.1163-08.2008

 0270-6474/08/286264-08$15.00/0

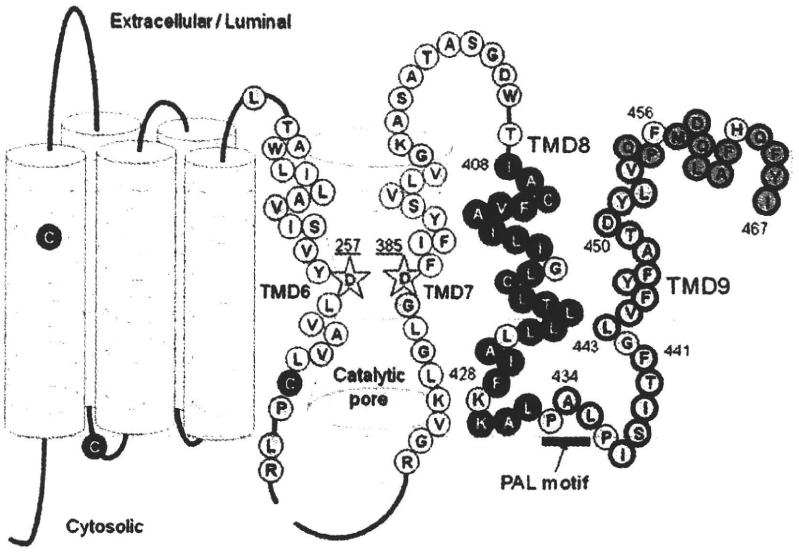

Figure 1. Locations of the PS1 cysteine mutations used in this study. A schematic depiction of human PS1 based on the nine-TMD topology model is shown. Catalytic aspartates are shown by yellow stars. Endogenous Cys residues that were replaced with serine in Cys-less PS1 are indicated as black circles. Amino acid residues substituted with Cys are shown by a circle with a single-letter character representing the original amino acids. Single-Cys mt was systematically substituted with residues in the predicted hydrophobic region 9, hydrophilic loop, hydrophobic region 10, and the C-terminal region, which are indicated by purple, blue, pink, and green circles, respectively. Cys substitutions that resulted in a loss of γ-secretase activity are indicated as gray circles.

have access to the catalytic site through a "lateral gate" facing a hydrophobic environment on the analogy of the translocon system (Lemberg and Martoglio, 2004; Lemberg and Freeman, 2007; Selkoe and Wolfe, 2007). However, no such functional domain has been identified within the γ-secretase, although pharmacological and chemical biological studies indicate the presence of a substrate binding site within γ-secretase that are distinct from the catalytic site (Esler et al., 2002; Das et al., 2003; Tian et al., 2003; Kornilova et al., 2005). In this study, we further analyzed the structure and the functional role of the more distal portion of the C-terminal fragment (CTF) of PS1, which contains two hydrophobic regions as well as the PAL motif, the latter being required for the proteolytic activity (Tomita et al., 2001; Wang et al., 2004).

Materials and Methods

Polyclonal antibody G1Nr5 was raised against recombinant human PS1 N terminus protein. G1L3, which recognizes a hydrophilic loop 6, was described previously (Tomita et al., 1999). Anti-CD44ICD, anti-$PS1_{NT}$ (Thinakaran et al., 1998), and PS-C3 (Honda et al., 1999) were kindly provided by Drs. H. Saya (Keio University, Shinjuku, Tokyo, Japan), G. Thinakaran (University of Chicago, Chicago, IL), and A. Takashima (RIKEN, Wako, Saitama, Japan), respectively. *N*-[*N*-(3,5-difluorophenacetyl)-L-alanyl]-(*S*)-phenylglycine *tert*-butyl ester (DAPT) was synthesized as described previously (Dovey et al., 2001; Kan et al., 2003). {1*S*-Benzyl-4*R*-[1-(1*S*-carbamoyl-2-phenylethylcarbamoyl)-1*S*-3-methylbutylcarbamoyl]-2*R*-hydroxy-5-phenylpentyl}carbamic acid *tert*-butyl ester (L-685,458) (Shearman et al., 2000) and peptide 15 (pep15) (Das et al., 2003) were purchased from Bachem and Ito Life Science, respectively. All 3-(4,5-dimethylthiazol-2-yl)-5-(3-carboxymethoxyphenyl)-2-(4-sulfophenyl)-2*H*-tetrazolium (MTS) reagents (Toronto Research Chemicals) were dissolved in DMSO at 200 mM before use or stored at −80°C until use. The abbreviations used for MTS cross-linkers are as follows: M2M, 1,2-ethanediyl bismethanethiosulfonate; M3M, 1,3-propanediyl bismethanethiosulfonate; M4M, 1,4-butanediyl bismethanethiosulfonate; M6M, 1,6-hexanediyl bismethanethiosulfonate; M8M, 3,6-dioxaoctane-1,8-diyl bismethanethiosulfonate; M11M, 3,6,9-trioxaundecane-1,11-diyl bismethanethiosulfonate; M14M, 3,6,9,12-tetraoxatetradecane-1,14-diyl bismethanethiosulfonate; M17M, 3,6,9,12,15-pentaoxaheptadecane-1,17-diyl bismethanethiosulfonate. cDNAs encoding APP_{NL}, PS1, and Cys-less PS1 were described previously (Sato et al., 2006). Single- or double-Cys mutant (mt) PS1 were generated using long PCR-based protocol. Maintenance of embryonic fibroblasts derived from *Psen1*/*Psen2* double knock-out (DKO) mouse cells (Herreman et al., 2000), retroviral infection system (Kitamura et al., 2003), and generation of stable infectants were done as previously described (Watanabe et al., 2005). Microsome preparation, immunoblot analysis, and quantitation of Aβ by two-site ELISAs were performed as previously described (Tomita et al., 1997, 1999, 2001; Hayashi et al., 2004). Biotinylation experiment using *N*-biotinylaminoethyl methanethiosulfonate (MTSEA-biotin) in intact cell (labeling from extracellular/luminal side) or microsome fraction (labeling from both extracellular/luminal and cytosolic sides) was performed as previously described (Sato et al., 2006; Isoo et al., 2007). The relative extents of biotinylation of PS1 fragments were calculated from the band intensities. For cross-linking experiments, resuspended microsomes incubated with MTS cross-linkers (10 mM) for 2 h at room temperature were mixed with sample buffer containing *N*-ethylmaleimide and then directly subjected to immunoblot analysis. For a competition assay, 2-sulfonatoethyl methanethiosulfonate (MTSES) or 2-(trimethylammonium)-ethyl methanethiosulfonate (MTSET) was preincubated with intact cells or microsomes for 15 min at room temperature and washed once before the biotinylation. γ-Secretase inhibitors were preincubated with intact cells or microsomes for 30 min at room temperature, before the biotinylation or cross-linking experiments. The inhibitors were used at concentrations that completely abolish the proteolytic activity of γ-secretase (Morohashi et al., 2006; Sato et al., 2006).

Results

SCAM analysis of hydrophobic region 9 and the PAL motif of PS1

Because of the relatively weak hydrophobicity of the hydrophobic region 10, the topology and geometry of the "TMD9" as well as of the extreme C terminus of PS1 had long been controversial. Recently, however, several cell-based topological studies revealed that the hydrophobic region 9 (I408–F428) and 10 (A434–V453) of PS1 (Henricson et al., 2005) penetrate the membrane as TMD8 and TMD9, respectively, and that the extreme C terminus is exposed to the extracellular/luminal side (Laudon et al., 2005; Oh and Turner, 2005; Spasic et al., 2006). Moreover, the PAL motif that resides at the N-terminal region of the hydrophobic region 10 is highly conserved in PS and SPP proteins and is required for the enzymatic activity (Tomita et al., 2001; Wang et al., 2004; Nakaya et al., 2005; J. Wang et al., 2006), although the mechanistic role of this motif remains unknown. To analyze the water accessibility of these regions, we first generated mutant PS1 carrying a single cysteine in Cys-less PS1 (single-Cys mt PS1) at 34 consecutive amino acid residues in and around the hydrophobic region 9 and PAL motif (I408–F441) (Fig. 1). Cys substitution of some residues abolished the expression or endoproteolysis of PS1 polypeptides, or Aβ generation (i.e., G417C, L425C, K429C, P433C, and P436C) (supplemental Fig. 1*A*,*D*, available at www.

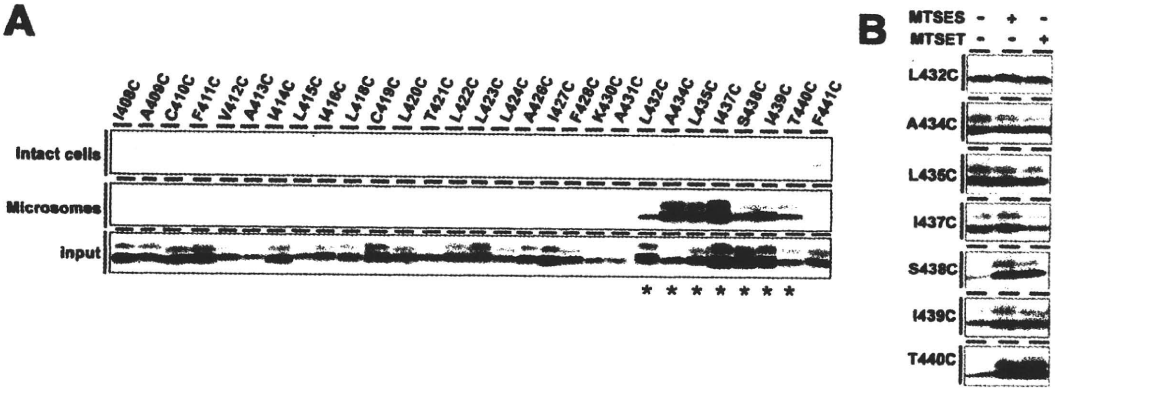

Figure 2. SCAM analysis of single-Cys mt PS1 in the hydrophobic region 9 and the PAL motif. ***A***, Biotin-labeling experiment using MTSEA-biotin in intact cells (top) and microsomes (middle). Bottom, Amount of PS1 CTF in the input fraction. Biotinylated mutants are indicated by asterisks below the panel. ***B***, Labeling competition by MTSES and MTSET was performed using microsomes. Locations of Cys mutations are shown on the left.

jneurosci.org as supplemental material). No single-Cys mt PS1 that harbored the γ-secretase activity as a holoprotein have so far been identified. Consistent with the previous results, mutants at the PAL motif (i.e., P433C and P436C) lost γ-secretase activity, which were excluded from further structural analyses. SCAM analysis of the remaining "active" single-Cys mt in intact cells revealed that none of the mutants were biotinylated by MTSEA-biotin from the extracellular side (Fig. 2*A*; supplemental Fig. 2*A*, available at www.jneurosci.org as supplemental material). We next examined the microsome labeling of single-Cys mt PS1 and found that all single-Cys mt PS1 starting from L432C to T440C were biotinylated, whereas no other mutants were labeled. Next, we examined the effects of other membrane-impermeable MTS derivatives, i.e., the negatively charged MTSES and the bulkier, positively charged MTSET, to analyze the steric and electrostatic environment around the biotinylated residues. The labeling of I437C by MTSEA-biotin was decreased by preincubation with MTSET, suggesting that I437 faces an open hydrophilic environment (Fig. 2*B*). However, preincubation with the charged MTS derivatives did not decrease the biotinylation of A434C, L435C, S438C, I439C, or T440C. These data suggest that all residues within the hydrophobic region 9 are inaccessible to water and face the hydrophobic environment as membrane-embedded TMD8. In contrast, the consecutive residues around the PAL motif (L432–T440) sit in a narrow, water-accessible cleft that is exclusively accessible from the cytosolic side.

SCAM analysis of hydrophobic region 10 and the extreme C terminus of PS1

We further generated single-Cys mt PS1 at 26 consecutive amino acid residues starting from the remaining C-terminal half of the hydrophobic region 10 to the extreme C terminus of PS1 (G442–I467) (Fig. 1). Again, some mutants (i.e., G442C, F456C, and H463C) lost the protein expression or γ-secretase activity and thus were excluded from further analyses (supplemental Fig. 1*B*,*D*, available at www.jneurosci.org as supplemental material). Labeling experiments using intact cells revealed that L443C, Y446C, D450C, Y451C, Q454C, D458C, Q459C, A461C, F462C, and Q464C were reactive with MTSEA-biotin from the extracellular side (Fig. 3*A*; supplemental Fig. 2*B*, available at www.jneurosci.org as supplemental material). Moreover, the labeling of D450C, Y451C, Q454C, D458C, Q459C, F462C, and Q464C were inhibited by preincubation with MTSES or MTSET, suggesting that the region C-terminal to D450, except for A461, faces

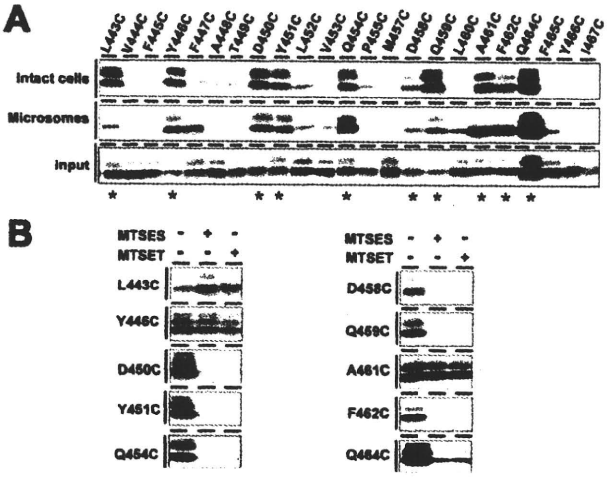

Figure 3. SCAM analysis of single-Cys mt PS1 around the hydrophobic region 10 and the extreme C terminus. ***A***, Biotin-labeling experiment using MTSEA-biotin in intact cells (top) and microsomes (middle). Bottom, Amount of PS1 CTF in the input fraction. Biotinylated mutants are indicated by asterisks below the panel. ***B***, Labeling competition by MTSES and MTSET was performed using intact cells. Locations of Cys mutations are shown on the left.

an open hydrophilic environment (Fig. 3*B*). In contrast, the biotinylation of L443C, Y446C, and A461C was not decreased by preincubation with the charged MTS derivatives. We next prepared microsome fractions from DKO cells expressing single-Cys mt PS1 of the hydrophobic region 10 and subjected them to labeling experiments (Fig. 3*A*; supplemental Fig. 2*B*, available at www.jneurosci.org as supplemental material). All residues that were labeled in intact cells were biotinylated, whereas the accessibilities of some residues (i.e., F447C and L460C) were different from those by intact cell labeling. Given that the PAL motif was accessible exclusively from the cytosolic side, it is most reasonable to conclude that the hydrophobic region 10 spans the membrane as TMD9 in the active γ-secretase complex, and that several residues at the C terminus of PS1 are exposed to the extracellular side.

Cross-linking experiments using MTS cross-linkers

We have previously found that TMD6 and TMD7 are located in close proximity within the catalytic pore, because L250C and I387C were directly cross-linkable (Sato et al., 2006). To gain

Table 1. Summary of the cross-linking experiments in double-Cys PS1 mt using different lengths of MTS cross-linkers

	MTS cross-linker	Distance (Å)
L250C/L432C (PAL)	-	
L250C/L435C (PAL)	M2M	≤5.2
L250C/L443C (TMD9)	M2M	≤5.2
L250C/Y446C (TMD9)	M8M	≤16.9
L250C/D450C (TMD9)	M17M	≤24.7
L250C/Q454C (TMD9)	No activity	
L250C/D458C (C-term)	-	
L250C/Q459C (C-term)	-	
L250C/A461C (C-term)	-	
A260C/L443C (TMD9)	No activity	

"MTS cross-linkers" indicate the abbreviated name of the shortest cross-linker that enabled the production of an NTF–CTF heterodimer (e.g., M2M). "-" represents the absence of the heterodimer formation by any cross-linkers. "Distance" indicates the length of the spacer arm of the MTS cross-linkers. C-term, Most C-terminal region. "No activity" indicates PS1 mutants that lack γ-secretase activity.

more insights into the structural characteristics of the C-terminal region in relation to the catalytic pore, we performed a systematic cross-linking experiment using MTS cross-linkers. M2M, M3M, M4M, M6M, M8M, M11M, M14M, and M17M are sulfhydryl-to-sulfhydryl cross-linking reagents with spacer arms of 5.2, 6.5, 7.8, 10.4, 13, 16.9, 20.8, and 24.7 Å long, respectively (Loo and Clarke, 2001b). First, cross-linking experiments using microsome fractions revealed that a subset of longer cross-linkers caused slow migration of N-terminal fragment (NTF) or CTF of single-Cys mt PS1 (L250C, A260C, L383C, I387C, and L435C) (supplemental Fig. 3*A–E*, available at www.jneurosci.org as supplemental material). No cross-linked products were observed in the following single-Cys mt: L432C, Y446C, and D450C (data not shown). Immunoblot analysis using single-Cys mt PS1 carrying M292D, which remains as a holoprotein (Steiner et al., 1999), revealed that these shifts neither represent the formation of homodimer of PS fragments nor the cross-linking of other components (i.e., nicastrin, Aph-1, and Pen-2) with PS1 (data not shown). The cross-linked products of ~20 kDa with CTF in L383C, I387C, and L435C mutants were decreased by preincubation with L-685,458 (supplemental Fig. 4, available at www.jneurosci.org as supplemental material). However, no antibodies against representative substrates of γ-secretase (i.e., APP, Notch, and CD44) reacted with this cross-linked product. These bands might represent the cross-linking of PS1 CTF with the endogenous unknown γ-secretase substrates or binding proteins harboring Cys. The characterization of these cross-linked proteins is underway.

We next generated a series of double-Cys mutant PS1 harboring a pair of Cys, located in NTF and CTF, respectively, in a single molecule (e.g., L250C/Y446C) in an attempt to locate TMD9 and the extreme C terminus relative to TMD6 (i.e., L250 and A260; summarized in Table 1). We chose several residues (i.e., around the PAL motif: L432 and L435; TMD9: L443, Y446, D450, and Q454; C terminus: D458, Q459, and A461) to examine the *in cis*-cross-linking with Cys introduced into TMD6 (i.e., L250 or A260). All double-Cys mutants retained γ-secretase activity except for L250C/Q454C and A260C/L443C, and only the active mutants were subjected to further cross-linking analyses (supplemental Fig. 1*C*, available at www.jneurosci.org as supplemental material). Coincubation of L250C/L435C, L250C/L443C, L250C/Y446C, and L250C/D450C double-Cys mutants with MTS cross-linkers decreased the amount of NTF and CTF, whereas a band close in size to that of a holoprotein (~45 kDa) emerged [Fig. 4, arrows; supplemental Fig. 5 (arrows), available at www.jneurosci.org as supplemental material]. These bands reacted with both anti-PS1 N- and C-terminal antibodies, but not with antibodies to other γ-secretase components (data not shown). The same results were obtained using two different antibodies for PS1 NTF and CTF (i.e., G1Nr5 and PS1NT for NTF, G1L3 and PS-C3 for CTF), suggesting that these polypeptides correspond to an NTF–CTF heterodimer, as previously observed (Sato et al., 2006). Notably, in L250C/L435C and L250C/L443C, NTF–CTF heterodimer was formed by M2M with a spacer arm of only 5.2 Å. Longer cross-linkers, e.g., M8M and M17M, were required for the NTF–CTF cross-linking in L250C/Y446C and L250C/D450C, respectively. In contrast, L432, D458, Q459, and A461 were not cross-linked to L250 (supplemental Fig. 6*A–H*, available at www.jneurosci.org as supplemental material). Collectively, these data indicate that the PAL motif and L443 in the middle of TMD9 are located in close proximity to TMD6 (i.e., ≤5.2 Å apart), and face the same hydrophilic pore.

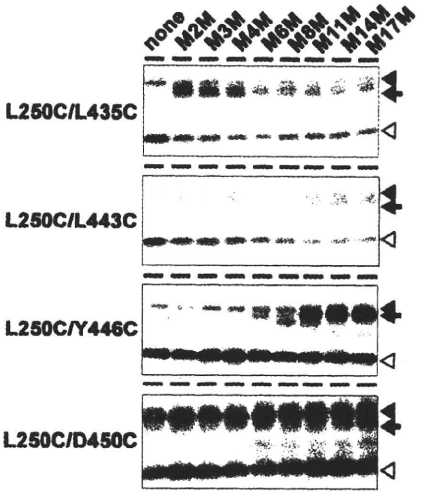

Figure 4. Cross-linking experiment using MTS cross-linkers. Cross-linking experiments of double-Cys mt in microsomes and immunoblot analysis using anti-$PS1_{NT}$ antibody. Locations of Cys mutations are shown on the left. PS1 full-length protein, NTF, and cross-linked product (NTF–CTF heterodimer) are shown by black arrowheads, white arrowheads, and black arrows, respectively.

Reactivity of substituted cysteines in the presence of γ-secretase inhibitors

Transition-state analog-type aspartyl protease inhibitors that target to the catalytic aspartates directly bind PS1 NTF and CTF (Li et al., 2000; Shearman et al., 2000; Esler et al., 2002). Helical peptide-based inhibitors mimicking the TMD structure bind PS fragments as well, but are unable to compete for the binding of transition-state analog inhibitors (Das et al., 2003; Kornilova et al., 2005). The dipeptidic inhibitor, DAPT, targets PS1 CTF in yet a third manner, and its binding site appears to be distinct from, but overlap with, that of transition-state analogues and helical peptides, suggesting that DAPT binds to a site involved in the substrate transfer (Kornilova et al., 2003, 2005; Micchelli et al., 2003; Morohashi et al., 2006). To examine the different binding sites for different types of inhibitors as well as the potential conformational changes that take place during their binding, we analyzed the accessibility of substituted Cys in the presence of representative γ-secretase inhibitors [i.e., transition-state analog (L-685,458), helical peptide (pep15), and dipeptidic compound (DAPT)].

The competition assays revealed that the accessibility of a se-

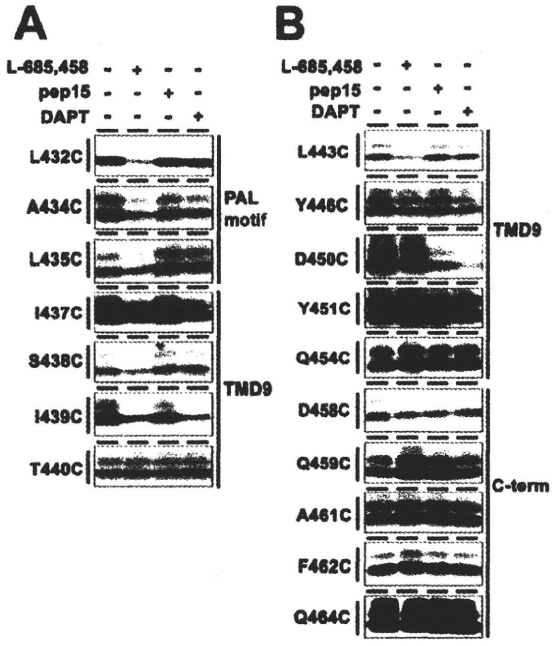

Figure 5. Labeling competition by γ-secretase inhibitors. ***A***, ***B***, Biotin labeling of single-Cys mt PS1 was conducted after preincubation with L-685,458, pep15, or DAPT in microsomes (***A***) or intact cells (***B***). Locations and predicted topology of Cys mutations are shown on the left and right, respectively.

ries of single-Cys mt PS1 around the PAL motif (L432C, A434C, L435C, I437C, S438C, and I439C) was significantly reduced by preincubation with L-685,458 (Fig. 5*A*). Moreover, the labeling of several L-685,458-sensitive residues (i.e., I437C, S438C, and I439C) was decreased by preincubation with DAPT, too. In contrast, the biotinylation of TMD9 and the extreme C terminus from the extracellular side was not affected by any of the γ-secretase inhibitors, except for L443C and D450C: the labeling of L443C was significantly and exclusively reduced by preincubation with L-685,458, whereas the biotinylation of D450C was sensitive to preincubation with pep15 and DAPT, but not with L-685,458 (Fig. 5*B*). It is well established that TMDs of several receptors and transporters rotate to cause structural rearrangements after treatment by agonists or antagonists (Horenstein et al., 2001; Loo and Clarke, 2001a). However, we observed no labeling of additional single-Cys mt PS1 that had originally been inaccessible to MTSEA-biotin under a condition in which the activity of γ-secretase is completely inhibited (data not shown). Therefore, it may be reasonable to speculate that the γ-secretase inhibitors tested here did not cause a rotation of TMDs. Altogether, our SCAM approach identified that the water accessibility of certain residues in PS1 is competed by various types of γ-secretase inhibitors, whose competition profiles were different from each other.

Discussion

The structure of the C-terminal region of PS1 in an active γ-secretase complex

In this study, we applied SCAM, in combination with cross-linking experiments, to the identification of amino acid residues in the C-terminal region of PS1 that are water accessible from either side of the membrane (Fig. 6*A*). None of the residues around the hydrophobic region 9 (I408–A431) showed water accessibility, suggesting that they are buried within the lipid bilayer as an authentic TMD (TMD8) and do not participate in the formation of the hydrophilic pore. In contrast, the consecutive residues around the PAL motif (L432–T440) were water accessible, but mostly with limited access. We speculate that this region sits in a narrow hydrophilic cleft that is only accessible from the cytosolic side, forming a v-shaped hydrophilic structure with I437 at the outermost tip. The cross-linking experiments revealed that this structure is located very close to the catalytic site within the pore. Notably, among the Cys mutants in TMD8 and TMD9, G417C and G442C lost the γ-secretase activity. Glycine is known as a "helix-breaking" residue for TMDs and gives helix flexibility in the lipid bilayer (Li and Deber, 1994; Ulmschneider and Sansom, 2001). Moreover, these glycines are almost completely conserved in PS homologues identified so far (supplemental Fig. 7, available at www.jneurosci.org as supplemental material). We speculate that TMD8 forms a bending structure at G417, which may be required for the γ-secretase activity. G442 may also form a hinge in the middle of TMD9 to provide the PAL motif and the extracellular/luminal half of TMD9 with flexibility.

Several residues within the extracellular/luminal side of TMD9 (G442-Q454) were highly hydrophilic: L443 and Y446 were water accessible with steric restrictions; D450, Y451, and Q454 were facing the hydrophilic environment, but with unlimited access. Importantly, all these residues were located on the same interface in an α-helical model (Fig. 6*B*). Moreover, the cross-linking experiments revealed that L443, Y446, and D450 were located in proximity to TMD6, suggesting that these residues face the catalytic pore. Of note, the minimum "cross-linkable" distances to L250 of these residues increased toward the C terminus. These data suggest that the luminal half of TMD9 forms a short α-helix that faces the catalytic pore, which is tilted away from the pore.

D458, Q459, A461, F462, and Q464 at the C terminus of PS1 also exhibited unlimited water access with the exception of A461. These residues were aligned on the same surface in an α-helical model, but in a surface different from that formed by the extracellular/luminal half of TMD9 (Fig. 6*B*). These surfaces appear to be connected by a proline that generates a helix kink (von Heijne, 1991). In contrast, the residues predicted to locate at the opposite side of the helix showed no water accessibility. This proline is highly conserved among species, suggesting the functional importance of the proline residue. After a kink at P455, the C terminus of PS1 (i.e., F456-Q464) may form a membrane-associated, short amphipathic α-helix that faces an aqueous environment. Interestingly, Cys substitution of F456, located next to P455 and also highly conserved, lost the γ-secretase activity. Phenylalanine is frequently found at the interface between the hydrophobic core and the phosphate region of the lipid (Killian and von Heijne, 2000). Furthermore, the extreme C terminus of PS1 (i.e., F465–I467) were located in a hydrophobic environment. This is in agreement with the previous finding that the relative hydrophobicity of these C-terminal residues is required for the interaction of PS1 with the TMD of nicastrin and the activity of γ-secretase, supporting the view that they are buried within the membrane (Bergman et al., 2004; Kaether et al., 2004). Thus, we speculate that the C-terminal short helix is tethered to the lipid bilayer by virtue of the hydrophobic nature of the extreme C terminus. This structure is reminiscent of a "slide helix," an amphipathic feature that contributes to the control of the conformation and activity of Kir6.2 potassium channels (Antcliff et al., 2005; Enkvetchakul et al., 2007). Notably, sequential deletion of the C-terminal residues of PS1 gradually decreased the γ-secretase activity, and the deletion of residues 451–467, which

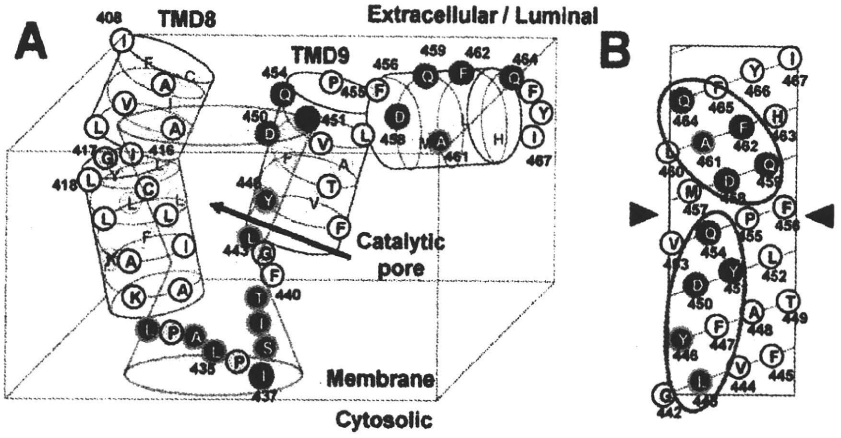

Figure 6. Hypothetical structure around TMD8, TMD9, and the extreme C terminus of PS1 revealed in this study. ***A***, Summary of SCAM analysis and a schematic depiction of the configuration of the TMD8 and TMD9 in relation to the catalytic pore. Cys mutants that were labeled by MTSEA-biotin are shown by a white letter in a black circle. Residues whose labeling was effectively competed by MTSES or MTSET are shown in a blue frame, and the unaffected residues are in a green frame. Residues that were not labeled by MTSEA-biotin or not analyzed are shown by black letters in white and gray circles, respectively. ***B***, An α-helical net representation of the C terminus of human PS1 starting at the N-terminal glycine 442. Consecutive hydrophilic surfaces are shown by orange circles. An arrowhead indicates a putative helix kink.

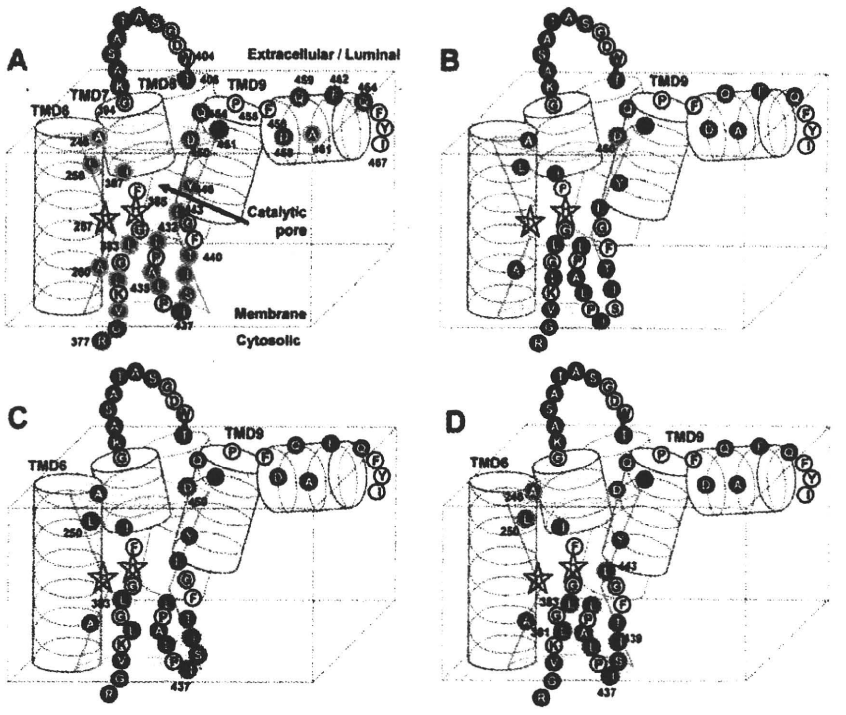

Figure 7. The model of the catalytic pore of γ-secretase and the locations of γ-secretase inhibitor-sensitive residues in PS1. ***A***, Schematic depiction of the structure around the catalytic pore coupled with our previous result (Sato et al., 2006) in the same manner as that in Figure 6*A*. Residues whose labeling was diminished by the presence of pep15 (***B***), DAPT (***C***), and L-685,458 (***D***) are shown in cyan, pink, and orange frames, respectively.

correspond to the amphipathic region identified here, totally abolished the activity (Tomita et al., 1999; Bergman et al., 2004), implicating the auxiliary role of the short C-terminal helix in the assembly and activity of γ-secretase.

Implications for the mechanism of intramembrane proteolysis

Several lines of evidence suggest that the intramembrane proteolysis is executed by the following consecutive steps: (1) binding of the substrate to the initial docking site, (2) substrate transfer to the catalytic environment through the lateral gate, and (3) hydrolysis of the scissile bond. By a series of competition assays using pharmacologically well characterized inhibitors, we identified a set of amino acid residues within PS1 that may play critical roles in the proteolytic mechanism (Fig. 7).

To examine the structural changes after substrate binding and to locate the substrate binding site, we performed a competition assay using the helical peptide-type inhibitor that is predicted to directly target the initial binding site, which may presumably reside in the interface of PS1 NTF/CTF (Das et al., 2003; Kornilova et al., 2005). The labeling of D450C by MTSEA-biotin was inhibited by preincubation with pep15 and DAPT, but not with L-685,458 (Fig. 7*B*). However, pep15 had no effect on the biotinylation of any other Cys mutants. Notably, the extracellular/luminal half of TMD9 harboring D450 appears to form a membrane-embedded short α-helix partitioned by the helix-breaking residues and face the hydrophilic catalytic pore. Strikingly, Cys mutants located at the hydrophobic helical interface on this region (i.e., V444C, A448C, and I453C) resulted in the augmentation of enzymatic activity (supplemental Fig. 1, available at www.jneurosci.org as supplemental material). This whole structure is highly reminiscent of TMD5 of rhomboid that faces the catalytic cavity and is supposed to constitute the lateral gate for substrate entry (Baker et al., 2007). Of note, loosening the hydrophobic interaction between TMD2 and TMD5 of rhomboid enhanced the proteolytic activity. Together, these results indicate that D450 and the extracellular/luminal helix of TMD9 of PS1 may comprise a part of the initial docking site or the lateral gate for substrate.

DAPT competed for labeling of Cys residues located C-terminal to the PAL motif (I437C, S438C, and I439C) as well as of D450C, all of which are located in close proximity to the catalytic pore (Fig. 7*C*). Consistent with the previous pharmacological results, the biotinylation of all DAPT-sensitive residues was diminished by preincubation of L-685,458 or pep15. It is noteworthy that DAPT has been shown to exhibit an inhibitor profile specific to γ-secretase and directly target the PS1 CTF, despite that γ-secretase and SPP share the GxGD and the PAL motif (Morohashi et al., 2006; Fuwa et al., 2007). Intriguingly, the DAPT-sensitive residues identified in this study (i.e., I437, S438, I439, and D450) are not conserved in SPP. Thus, we hypothesize that these residues comprise a protein surface for the DAPT binding site that had been shown to reside within the PS1 CTF. Fur-

ther competition analysis using dibenzazepine, a potent inhibitor that directly targets the PS1 NTF and SPP (Fuwa et al., 2007), would provide more precise pharmacostructural information about this point.

The PAL motif is reported to be critical for γ-secretase activity and the binding of the transition state analog inhibitor L-685,458 (J. Wang et al., 2006). Consistent with this notion, the labeling of consecutive residues around the PAL motif, as well as of L443 in TMD9, were inhibited by preincubation with L-685,458 (Fig. 7*D*). Moreover, the cross-linking study revealed that all these regions are located in close proximity around the catalytic aspartates. Importantly, mutagenesis studies revealed that the replacement of P433 or A434 with tiny amino acid residues (e.g., Ala, Gly, and Ser) was tolerated for the preservation of the γ-secretase activity, whereas substitution of P433 with bulky amino acids (e.g., Val, Leu, or Ile) abolished the activity (Nakaya et al., 2005; J. Wang et al., 2006). These results favor the notion that the requirement of the PAL motif in intramembrane proteolysis is independent of the proline-mediated reverse turn structure or the hydrophobicity. Together with our finding, we propose that the hydrophilic and smooth surface structure formed by the residues around the PAL motif directly functions as a subsite and constitutes the "catalytic plug" within the pore together with the GxGD motif (Sato et al., 2006).

Based on the results of SCAM analysis in combination with the competition assay using mechanism-based γ-secretase inhibitors, we propose the functional role of PS1 in the intramembrane proteolysis as follows (supplemental Fig. 8, available at www.jneurosci.org as supplemental material). The substrate (1) initially binds to the extracellular/luminal helix of TMD9 that comprises the lateral gate, (2) is transferred through the C-terminal side of the PAL motif, and (3) is recruited to the catalytic site composed of the extracellular/luminal half of TMD6, the GxGD motif, the PAL motif, and the N-terminal end of TMD9. However, we are not able to exclude the possibility that the binding of inhibitors caused conformational changes that made the Cys residue inaccessible to water. Nonetheless, further SCAM analysis, as well as other biochemical and structural studies, will reveal the whole picture of the γ-secretase cleavage, in which substrates are introduced through the lateral gate and subjected to cleavage within the hydrophilic catalytic pore.

References

Antcliff JF, Haider S, Proks P, Sansom MS, Ashcroft FM (2005) Functional analysis of a structural model of the ATP-binding site of the KATP channel Kir6.2 subunit. EMBO J 24:229–239.

Baker RP, Young K, Feng L, Shi Y, Urban S (2007) Enzymatic analysis of a rhomboid intramembrane protease implicates transmembrane helix 5 as the lateral substrate gate. Proc Natl Acad Sci USA 104:8257–8262.

Bergman A, Laudon H, Winblad B, Lundkvist J, Näslund J (2004) The extreme C terminus of presenilin 1 is essential for γ-secretase complex assembly and activity. J Biol Chem 279:45564–45572.

Das C, Berezovska O, Diehl TS, Genet C, Buldyrev I, Tsai JY, Hyman BT, Wolfe MS (2003) Designed helical peptides inhibit an intramembrane protease. J Am Chem Soc 125:11794–11795.

Dovey HF, John V, Anderson JP, Chen LZ, de Saint Andrieu P, Fang LY, Freedman SB, Folmer B, Goldbach E, Holsztynska EJ, Hu KL, Johnson-Wood KL, Kennedy SL, Kholodenko D, Knops JE, Latimer LH, Lee M, Liao Z, Lieberburg IM, Motter RN, et al. (2001) Functional γ-secretase inhibitors reduce β-amyloid peptide levels in brain. J Neurochem 76:173–181.

Enkvetchakul D, Jeliazkova I, Bhattacharyya J, Nichols CG (2007) Control of inward rectifier K channel activity by lipid tethering of cytoplasmic domains. J Gen Physiol 130:329–334.

Esler WP, Kimberly WT, Ostaszewski BL, Ye W, Diehl TS, Selkoe DJ, Wolfe MS (2002) Activity-dependent isolation of the presenilin-γ-secretase complex reveals nicastrin and a γ substrate. Proc Natl Acad Sci USA 99:2720–2725.

Feng L, Yan H, Wu Z, Yan N, Wang Z, Jeffrey PD, Shi Y (2007) Structure of a site-2 protease family intramembrane metalloprotease. Science 318:1608–1612.

Fuwa H, Takahashi Y, Konno Y, Watanabe N, Miyashita H, Sasaki M, Natsugari H, Kan T, Fukuyama T, Tomita T, Iwatsubo T (2007) Divergent synthesis of multifunctional molecular probes to elucidate the enzyme specificity of dipeptidic γ-secretase inhibitors. ACS Chem Biol 2:408–418.

Hayashi I, Urano Y, Fukuda R, Isoo N, Kodama T, Hamakubo T, Tomita T, Iwatsubo T (2004) Selective reconstitution and recovery of functional γ-secretase complex on budded baculovirus particles. J Biol Chem 279:38040–38046.

Henricson A, Käll L, Sonnhammer EL (2005) A novel transmembrane topology of presenilin based on reconciling experimental and computational evidence. FEBS J 272:2727–2733.

Herreman A, Serneels L, Annaert W, Collen D, Schoonjans L, De Strooper B (2000) Total inactivation of γ-secretase activity in presenilin-deficient embryonic stem cells. Nat Cell Biol 2:461–462.

Honda T, Yasutake K, Nihonmatsu N, Mercken M, Takahashi H, Murayama O, Murayama M, Sato K, Omori A, Tsubuki S, Saido TC, Takashima A (1999) Dual roles of proteasome in the metabolism of presenilin 1. J Neurochem 72:255–261.

Horenstein J, Wagner DA, Czajkowski C, Akabas MH (2001) Protein mobility and GABA-induced conformational changes in GABA(A) receptor pore-lining M2 segment. Nat Neurosci 4:477–485.

Isoo N, Sato C, Miyashita H, Shinohara M, Takasugi N, Morohashi Y, Tsuji S, Tomita T, Iwatsubo T (2007) Abeta42 overproduction associated with structural changes in the catalytic pore of γ-secretase: common effects of Pen-2 N-terminal elongation and fenofibrate. J Biol Chem 282:12388–12396.

Kaback HR, Sahin-Tóth M, Weinglass AB (2001) The kamikaze approach to membrane transport. Nat Rev Mol Cell Biol 2:610–620.

Kaether C, Capell A, Edbauer D, Winkler E, Novak B, Steiner H, Haass C (2004) The presenilin C-terminus is required for ER-retention, nicastrin-binding and gamma-secretase activity. EMBO J 23:4738–4748.

Kan T, Tominari Y, Morohashi Y, Natsugari H, Tomita T, Iwatsubo T, Fukuyama T (2003) Solid-phase synthesis of photoaffinity probes: highly efficient incorporation of biotin-tag and cross-linking group. Chem Commun 7:2244–2245.

Karlin A, Akabas MH (1998) Substituted-cysteine accessibility method. Methods Enzymol 293:123–145.

Killian JA, von Heijne G (2000) How proteins adapt to a membrane-water interface. Trends Biochem Sci 25:429–434.

Kitamura T, Koshino Y, Shibata F, Oki T, Nakajima H, Nosaka T, Kumagai H (2003) Retrovirus-mediated gene transfer and expression cloning: powerful tools in functional genomics. Exp Hematol 31:1007–1014.

Kornilova AY, Das C, Wolfe MS (2003) Differential effects of inhibitors on the γ-secretase complex. Mechanistic implications. J Biol Chem 278:16470–16473.

Kornilova AY, Bihel F, Das C, Wolfe MS (2005) The initial substrate-binding site of γ-secretase is located on presenilin near the active site. Proc Natl Acad Sci USA 102:3230–3235.

Laudon H, Hansson EM, Melén K, Bergman A, farmery MR, Winblad B, Lendahl U, von Heijne G, Näslund J (2005) A nine-transmembrane domain topology for presenilin I. J Biol chem 280:35352-35360.

Lazarov VK, Fraering PC, Ye W, Wolfe MS, Selkoe DJ, Li H (2006) Electron microscopic structure of purified, active γ-secretase reveals an aqueous intramembrane chamber and two pores. Proc Natl Acad Sci USA 103:6889–6894.

Lemberg MK, Freeman M (2007) Cutting proteins within lipid bilayers: rhomboid structure and mechanism. Mol Cell 28:930–940.

Lemberg MK, Martoglio B (2004) On the mechanism of SPP-catalysed intramembrane proteolysis; conformational control of peptide bond hydrolysis in the plane of the membrane. FEBS Lett 564:213–218.

Li SC, Deber CM (1994) A measure of helical propensity for amino acids in membrane environments. Nat Struct Biol 1:368–373.

Li YM, Xu M, Lai MT, Huang Q, Castro JL, DiMuzio-Mower J, Harrison T, Lellis C, Nadin A, Neduvelil JG, Register RB, Sardana MK, Shearman MS, Smith AL, Shi XP, Yin KC, Shafer JA, Gardell SJ (2000) Photoactivated